

Gene-Mating Dynamic Evolution Theory: fundamental assumptions, exactly solvable models and analytic solutions

Juven C. Wang^{1,2,*} and Jiunn-Wei Chen^{3,†}

¹*Department of Physics, Massachusetts Institute of Technology, Cambridge, MA 02139, USA*

²*Perimeter Institute for Theoretical Physics, Waterloo, ON, N2L 2Y5, Canada*

³*Department of Physics, National Taiwan University and National Center for Theoretical Sciences,
and Leung Center for Cosmology and Particle Astrophysics, Taipei 10617, Taiwan*

(Dated: Work completed in 2006. Work reported in 2014.)

Fundamental properties of macroscopic gene-mating dynamic evolutionary systems are investigated. A model is studied to describe a large class of systems within population genetics. We focus on a single locus, any number of alleles in a two-gender dioecious population. Our governing equations are time-dependent continuous differential equations labeled by a set of parameters, where each parameter stands for a population percentage carrying certain common genotypes. The full parameter space consists of all allowed parameters of these genotype frequencies. Our equations are uniquely derived from four fundamental assumptions within any population: (1) a closed system; (2) average-and-random mating process (mean-field behavior); (3) Mendelian inheritance; (4) exponential growth and exponential death. Even though our equations are nonlinear with time-evolutionary dynamics, we have obtained an exact analytic time-dependent solution — we have an exactly solvable model. Our findings are summarized from phenomenological and mathematical viewpoints. From the phenomenological viewpoint, any initial parameter of genotype frequencies of a closed system will eventually approach a stable fixed point. Under time evolution, we show (1) the monotonic behavior of genotype frequencies, (2) any genotype or allele that appears in the population will never become extinct, (3) the Hardy-Weinberg law, and (4) the global stability without chaos in the parameter space. To demonstrate the experimental evidence for our theory, as an example, we show a mapping from the data of blood type genotype frequencies of world ethnic groups to our stable fixed-point solutions. From the mathematical viewpoint, our highly symmetric governing equations result in continuous global stable equilibrium solutions: these solutions altogether consist of a continuous curved manifold as a subspace of the whole parameter space of genotype frequencies. This fixed-point manifold is a global stable attractor, attracting any initial point in any Euclidean fiber to the fixed point where this fiber is attached. The stable base manifold and its attached fibers form a fiber bundle, which fill in the whole genotype frequency space completely. We can define the genetic distance of two populations as their geodesic distance on the equilibrium manifold. In addition, the modification of our theory under the process of natural selection and mutation is addressed.

PACS numbers: 87.10.-e, 87.23.-n, 83.80.Lz, 05.45.-a

CONTENTS

I. Introduction	2	1. Governing equations and exact analytic solutions	7
II. Four assumptions from fundamental views	4	2. Experimental evidence - data fitting	8
III. Model	4	3. Explanation and application of the chart - relations of different ethnic groups by geodesic distances	9
A. Model of 2 Alleles: 1 Dominant Gene and 1 Recessive Gene	4	IV. General Gene-Mating Evolution Model and Theory	16
1. Governing equations for population	4	A. Governing equations, stable equilibrium solutions and exact analytic solutions	16
2. Governing equations for percentages	5	B. 1-1 mapping and the well-defined manifold	17
3. Equilibrium solutions	5	C. Equilibrium solutions as a global attractor, monotonic behavior, non-extinction and the Hardy-Weinberg Law	17
4. From the linear stability analysis to the exact analytic time-dependent dynamical solution	6	V. Mutation and Natural Selection	17
B. Model of 3 Alleles: 2 Dominant Genes and 1 Recessive Gene: Blood Type Evolution Model	7	VI. Conclusion	18
		VII. Acknowledgements	19
		References	19

* juven@mit.edu

† jwc@phys.ntu.edu.tw

I. INTRODUCTION

Time evolution of population percentages labeled by biological traits or genetic characteristics in a population system is a main subject of studies for population genetics and evolutionary biology ([1–6] and references therein). Their governing laws may involve classical genetics, which can be traced back to Mendel’s seminal work [7]. Both the birth rate and death rate of a system will change the population number. Also the mating mechanism and inheritance laws will determine the percentage weight of newborn biological traits. There are abundant past researches and advance studying population genetic questions and equations ([1–6]). For example, Wright and other pioneer researchers [1] favor use of discrete difference equations to label each generation and the reproduction. However, the difference equation does not manifest the dynamical properties as transparently as the continuous differential equations, pioneered by Fisher, Crow and Kimura, *et al.* [2, 3]. In this work, we will formulate a set of exactly solvable nonlinear differential equations with a first-order time derivative to address population genetic questions.

Out of curiosity, the authors had posed the following questions to ourselves many years ago [8]:

- How should we characterize an ecological or macroscopic biological system consisting of a large population of many living beings within a mathematical framework?
- How can we characterize the time-dependent evolution of genetic diversity and genotype percentage of a population driven by the mating process and population growth?
- Is there a mathematical definition of genetic distance between two population groups even within the same species under the biological taxonomy? For example, can we quantitatively define the mathematical genetic distance of different ethnic groups of Homo sapiens, human beings? What would be the genetic distance of ethnic groups: Taiwanese, Cantonese, Japanese, Jewish, Irish people, etc.? Similarly, can we quantitatively define the relative genetic distances of other animal or plant species (within the same species), such as Darwin’s finches, studied in Charles Darwin’s “*On the Origin of Species*” [9]?

To our amusement, however, even without any necessity of deep biological knowledge, we can independently derive, from scratch, a set of exactly solvable governing equations describing a universal large class of systems addressing the issues of population genetics and evolutionary biology:

- Our model contains time-dependent governing equa-

tions together with our four fundamental assumptions.

- Our theory incorporates exactly solvable models and their mathematical properties describing population genetic systems.
- Our theory provides an answer to each of the questions we posed above.

To the best of our knowledge, the analysis closest to ours in the literature is Ref.[10]. In Ref.[10], some exact solvable models within a gene pool are analyzed, where the monotonic evolutionary behavior is found. Our model is similar to Ref.[10]’s model: Ref.[10]’s studies a single locus for an arbitrary number of alleles with or without distinguishing the sex; we study a single locus, arbitrary number alleles in a two-gender dioecious population. Though Ref.[10] reaches results similar to ours, we find several new ingredients:

- (1) The stable equilibrium solutions as a manifold.
- (2) The parameterization of the equilibrium manifold.
- (3) The experimental evidence of the model, such as the blood type of human ethnic groups. We present the experimental data of phenotype ($O_{exp}, A_{exp}, B_{exp}, AB_{exp}$) in Table.I, III, IV. We present our corresponding theoretical prediction of genotype ($O_t, AA_t, Ai_t, BB_t, Bi_t, AB_i$) in Table.II, V, VI. See Sec.VIII for figures.
- (4) The proposal to define the genetic distance of two populations as their geodesic distance on the equilibrium manifold in the genotype frequency space.
- (5) The exact analytic solution in terms of a Euclidean fiber bundle.
- (6) Our work may be viewed as a unified framework combining the exact analytic solutions of Ref.[10] with the stability analysis of the Hardy-Weinberg law [11, 12], together with a proper parameterization of stable equilibrium manifold.

We believe that our work adds value to the literature.

We will work out our model step by step. To characterize a population genetic system, the first step is to find a good biological *parameter* to label the system. The biological trait can be a genotype or phenotype. Here we will use the genotype, the genetic makeup of an individual. The genotype contains a set of choices of possible alleles. We will focus on a genotype determined by a single locus and an arbitrary number of alleles. We will use the *genotype frequency*, the number of individuals with a given genotype normalized by the total number of individuals in the population. A set of genotype frequencies provides the *normalized parameter* to label the given population. Throughout the text, we may also term this *genotype frequency* concept as “*percentage parameter*” or simply “*parameter*” of the given population. The full parameter space consists of all allowed genotype frequencies of the population. Under governing principles, the genotype frequency can evolve under the time evolution.

In this work, we start from four fundamental assump-

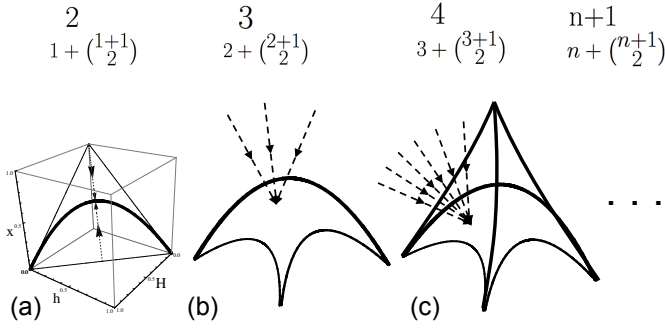


FIG. 1. The geometrical illustration of exact analytic solutions of our model, see Sec.III, Sec.IV for details. For a total number $(n + 1)$ of alleles, denoted as $n + 1$ in the top row, such as n dominant genes and 1 recessive gene. The full dimension of the whole *percentage parameter* space of genotype frequency is $n + \binom{n+1}{2}$, shown in the second row. The stable solutions altogether consist of a n -dimensional continuous curved manifold as a subspace of the whole parameter space. This n -dimensional fix-point manifold is a global stable attractor under time evolution, attracting any initial point in a $\binom{n+1}{2}$ -dimensional Euclidean fiber to the fixed point where this fiber is attached. The Euclidean fiber here is spanned by the dashed arrows, with its dimensionality of $\binom{n+1}{2}$: 1 in (a), 3 in (b), 6 in (c). The stable manifold and its attached fibers form the $n + \binom{n+1}{2}$ -dimensional fiber bundles, filling in the whole parameter space completely. Figure (a) illustrates the example presented in Sec.III A. Figure (b) illustrates the example presented in Sec.III B; Figure (c) illustrates a more generic case, presented in Sec.IV.

tions in Sec.II. In Sec.III, IV: we derive the dynamical governing equations under time evolution. We solve the time-dependent exact analytic solution (see Fig.1 for an illustration) from a set of coupled nonlinear differential equations with first-order time derivatives. We are able to show global stability, monotonic evolution, and no chaos for any population system. We prove that any genotype or allele that ever presents in the population will never become extinct and also derive the Hardy-Weinberg law [11, 12] in Sec.IV.

In addition to the analytical work, we also found experimental data strongly consistent with our study to confirm the validity of our theory. Specifically, we examine the experimental data of the genotype frequency of blood type [13] for (1) different ethnic groups and (2) different countries, in Sec.III B. With strong evidence and some expected error bars, the data can be rigorously fitted into our stable equilibrium solutions of governing equations. The stable equilibrium manifold can be mapped to a continuous two-dimensional quadrant map. This gives a panorama of how each ethnic group relates to another one. See FIG.2 for an illustration. Our result demonstrates that the laws of inheritance tend to approach stable equilibrium rather than with the usual chaos or complexity occurring in other nonlinear systems. In addition to this standard case, we further briefly analyze the case incorporating natural selection and mutation.

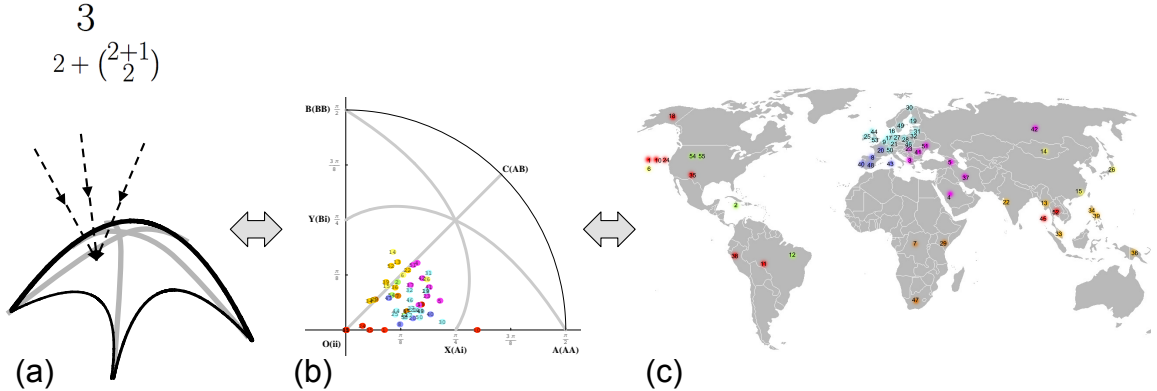


FIG. 2. Here we take the blood type evolution model (3 alleles) presented in Sec.III B as an example. In this work, we establish the mapping from (a) the stable equilibrium curved manifold (see Fig.1) to (b) the stable fixed-point quadrant parametrized by (θ_1, θ_2) defined in Sec.III B, see FIG.14,15. Our mapping parameterization may find its use for a correspondence to (c) the geographical map of ethnic groups in the world, see FIG.13. We can define the genetic distance of ethnic groups using the method presented in Sec.III B.

We anticipate that our analytical solutions may be a good starting basis for understanding more sophisticated models. With the experimental evidence between the the world-ethnic-group blood type genotype frequency

data and our stable solutions, we believe that our stable solutions and exact dynamical analytic solutions can be applied to other macroscopic population genetic systems (including human ethnic groups as well as other animals

or plants), as long as the system is approximately obeying the assumptions we made. We hope that our parameterization of analytic stable fixed-point solutions can be an efficient map to characterize the stabilized genotype frequencies. Our mapping may find its home in the textbooks of population genetics and evolutionary biology in the future.

II. FOUR ASSUMPTIONS FROM FUNDAMENTAL VIEWS

Here we start from scratch, by introducing the four fundamental assumptions used to construct our model. Our purpose lies in knowing how the genotype frequencies evolve under the mating process of a certain population system.

First, we focused on a system where the mating process is approximately **closed** inside itself. Hence, the newborn generation is totally a production from the old generation of the system. We should be aware that it does not matter whether the population locates together geographically. In this way, we could associate our model to different ethnic groups of humans, because the mating process of each ethnic group is approximately closed in each system. Hybrids between different ethnic groups are usually minorities compared to the majority ethnic groups.

Second, to determine the mating procedure, we assume the mating is overall **average and random**, which is intuitively reasonable under mean-field approximation. This assumption would not be far away from reality, considering the balance within an overall large population system. This assumption states no preference for the mating in a certain system. For example, we consider a system of n genotypes. Suppose P_i is the population amount of the genotype i , and assume a half-male-half-female population. The random mating mechanism of the male amount $P_k/2$ mates with all types of the female amount $P_i/2$ is $\frac{P_k}{2}(\sum \frac{P_i}{2}) = \frac{P_k}{2}(\sum \frac{P_i}{2})$, where P is the total population. We interpret this expression as the male amount multiplied by the probability to meet certain types of female. On the other hand, we have the female amount $P_k/2$ to meet all types of the male amount P_i . Notice that the interchangeable $P_k P_k$ term counts only once (male k with female k); however, $P_k P_j$ ($j \neq k$) counts twice (male k with female j , and male j with female k). The only mating dependence on a certain genotype is the population number of that genotype - if the population number for a certain genotype is large, then, it will have a greater chance to mate and also to be mated with by other genotype; and vice versa. Overall, this mechanism gives quadratic forms to the governing equations. The mating within the same ethnic groups or in a local geographical region plausibly obeys this second assumption.

Third, we consider the simplest inheritance law, the

classical genetics: Mendelian inheritance, to relate the transmission of hereditary traits (alleles) from the parents to the newborn generation. Although there is much new progress in genetics study, Mendelian inheritance is still a primary principle for capturing the main properties of heredity.

Fourth, in order to make the system dynamic under the time evolution, there must be a guideline for population growth. Here we consider the exponential growth — Malthusian growth model. Again, this law adumbrates the main feature of population growth with some acceptable deviations from the experiment. We will find later that these assumptions are beneficial for having analytically exactly solvable solutions.

One can apply the model to other animal or plant mating systems under a similar inheritance law, if it basically satisfies the above assumptions.

We summarize our **four assumptions** as follows:

- (a) The mating of gene-holders is (approximately) **closed** in a population system.
- (b) The mating probability for a certain genotype to another genotype, due to **average-and-random** mating mechanism, is proportional to the product of their population (quadratic form). It evolves under the **mean-field** assumption.
- (c) The probability of a genotype for the newborn generation obeys the **Mendelian inheritance**.
- (d) The accumulation of human population obeys the **exponential growth law**, for both the birth and the death processes.

We should be aware of the fourth assumption that the exponential growth includes the balance between the newborn and the dead. We denote the birth rate k_b and the death rate k_d . The overall net growth rate is $k = k_b - k_d$.

To derive the governing differential equations, implicitly we have another hidden assumption: the continuous limit. Throughout our work, we will take the continuous time t . The discrete positive integer population number can be treated approximately as a continuous real number in a large population.

III. MODEL

A. Model of 2 Alleles: 1 Dominant Gene and 1 Recessive Gene

1. Governing equations for population

We first consider the simplest model of our theory, which begins with two alleles and a single locus, such as one dominant gene A and one recessive gene a . We

take the hairstyle being curly or straight as an example, which roughly obeys this kind of inheritance law. Dominant gene A shows the curly property; only inheritance of no dominant gene shows the straight property. Curl hair owners indicate their genotype must be either AA or Aa . Straight hair owners' genotype must be aa . Below we denote the *population parameters*: H for AA , x for Aa , and h for aa . H stands for the number of people in the population carrying AA , x stands for the number of people in the population carrying Aa , and h stands for the number of people in the population carrying aa .

We now can write down the governing differential equations under a time t evolution of population number for hairstyle based on 4 assumptions in Sec.II:

$$\begin{cases} \frac{dH}{dt} = k_b \frac{1}{P} (H^2 + Hx + \frac{x^2}{4}) - k_d H, \\ \frac{dh}{dt} = k_b \frac{1}{P} (h^2 + hx + \frac{x^2}{4}) - k_d h, \\ \frac{dx}{dt} = k_b \frac{1}{P} (2Hh + Hx + hx + \frac{x^2}{2}) - k_d x. \end{cases} \quad (1)$$

We denote the total population to be $H + h + x = P$.

These equations have a first-order time derivative $\frac{d}{dt}$, associating the left-hand-side (LHS) population changes to the right-hand-side (RHS) birth and death effects. Linear terms on the RHS represent the death amount per unit time. Quadratic forms on the RHS represent the newborn population per unit time following Mendelian inheritance. Taking $\frac{H^2}{P}$ of $\frac{dH}{dt}$, for example, it represents our second assumption that the probability for male H to meet female H is $\frac{H}{P}$. The offspring of those parents is definitely H . So there must be a term $\frac{H^2}{P}$ in the RHS of the equation $\frac{dH}{dt}$, up to a constant factor. Now considering the Hx term, it can be either male H to meet female x , or male x to meet female H . So the overall effect must be $2Hx$ for the RHS newborn generation. The $2Hx$ is separated into two parts: Hx for $\frac{dH}{dt}$ and Hx for $\frac{dx}{dt}$, because Mendelian inheritance shows the offspring of H and x parents has a half probability to be H and another half to be x . Similarly, we can determine all the other coefficients of quadratic terms by the same arguments. The sum on the newborn part of the RHS must be all the possibilities for any pair of genes (alleles), $(H + h + x) \frac{(H + h + x)}{P}$, and this is equal to P . We notice that the sum of RHS is $\frac{dP}{dt}$, LHS is $(k_b - k_d)P$. This perfectly obeys assumption (d): $\frac{dP}{dt} = (k_b - k_d)P = kP$. We next check that the model is self-consistent, and uniquely determined by our four assumptions listed in Sec.II.

2. Governing equations for percentages

Now we revise our equations via normalizing each gene carrier population by the total population, using the *percentage parameters*, so called *genotype frequencies*. Consider, $\frac{d}{dt}(\frac{G}{P}) = \frac{1}{P} \frac{dG}{dt} - G \frac{dP/dt}{P^2}$, where G is any one of H, h, x . This turns out to be $\frac{d}{dt}(\frac{G}{P}) = \frac{1}{P} [k_b \frac{1}{P} (\text{quadratic form}) - k_d G] - G \frac{(k_b - k_d)P}{P^2} =$

$k_b (\frac{\text{quadratic form}}{P^2} - \frac{G}{P})$. Now by redefining $\frac{G}{P} \rightarrow G$, we have the governing equations for *genotype frequencies*:

$$\begin{cases} \frac{dH}{dt} = k_b (H^2 + Hx + \frac{x^2}{4} - H), \\ \frac{dh}{dt} = k_b (h^2 + hx + \frac{x^2}{4} - h), \\ \frac{dx}{dt} = k_b (2Hh + Hx + hx + \frac{x^2}{2} - x). \end{cases} \quad (2)$$

We notice that the death rate k_d takes no effect on the percentage governing equations. That is because the death effect does not rearrange the percentage parameters, every percentage parameter just universally dies away. Although the *population parameter* changes under death effect, the *genotype frequency* does not.

For both Eq.(1) and Eq.(2), there is a permutation symmetric group S_2 symmetry by exchanging $H \leftrightarrow h$.

3. Equilibrium solutions

We should be aware that there is a constraint $H + h + x = 1$, and the limited range for each parameter. The total degree of freedom is $3 - 1 = 2$. Namely the whole parameter space of *population parameters* are 3 dimensional, but the whole parameter space of *percentage parameters*, the *genotype frequencies*, are 2 dimensional.

Our aim is to realize the time evolution properties of this dynamical model. We first narrow down to see the equilibrium solution, which is the solution fixed in the parameter space without evolving under time evolution. The solution are solved by setting the RHS algebraic equations Eq.(2) to be zero. Among all expressions of the algebraic solution, we find the following one is the most appropriate representation:

$$\begin{cases} H_{eq}(\theta) = \frac{\cos^2(\theta)}{(\cos(\theta) + \sin(\theta))^2}, \\ h_{eq}(\theta) = \frac{\sin^2(\theta)}{(\cos(\theta) + \sin(\theta))^2}, \\ x_{eq}(\theta) = \frac{2 \sin(\theta) \cos(\theta)}{(\cos(\theta) + \sin(\theta))^2}. \end{cases} \quad (3)$$

It gives an one-to-one mapping between the equilibrium solution (H_{eq}, h_{eq}, x_{eq}) and θ , and shows the solution is a 1-dimensional continuous manifold. This representation also shows the symmetry of H and h in governing equations relates to the symmetry of H and h in equilibrium solution. The symmetry of $\theta_1 \leftrightarrow \frac{\pi}{2} - \theta_1$ relates to the S_2 symmetry of $H \leftrightarrow h$. The S_2 symmetry also results in a number of time-independent *conserved quantities* under Eq.(2). We find, for example, $\frac{d(H-h)}{dt} = \frac{d(2H+x)}{dt} = \frac{d(2h+x)}{dt} = 0$. By the constraint $H + h + x = 1$, the three quantities $H - h$, $2H + x$, and $2h + x$ are indeed the same equivalent conserved quantity. We can say the S_2 symmetry results in 1 *conserved quantity*, thus the dimensionality of fixed-point solutions is 1, here parametrized by θ .

4. From the linear stability analysis to the exact analytic time-dependent dynamical solution

By doing the linear stability analysis on the dynamical Eq.(2) with a small perturbation around this equilibrium solution Eq.(3), we find that it is stable with eigenvalues 0, -1 [14] for the entire two-dimensional parameter space. The first eigenvector for the eigenvalue 0 corresponds to the *marginal* tangent direction [14] of 1-dimensional equilibrium solution. Surprisingly, the second eigenvector for the eigenvalue 1 is *irrelevant and stable perturbation* [14] along the fixed direction $\hat{H} + \hat{h} - 2\hat{x}$. We define a new basis $\hat{s} = \hat{H} + \hat{h} - 2\hat{x}$, and s is the coordinate along \hat{s} .

It is well-known that nonlinear equations may have complicated global properties, such as chaotic behaviors. Usually the numerical simulation is required, and there are seldom cases which analytic solution for time evolution is exactly solvable. However, below we will show how to obtain the exact analytic time-dependent solution of Eq.(2). Our method is to change the description of parameters in Cartesian coordinates (H, h, x) to parameters in curvilinear coordinates (θ, s) . We transform H, h, x to θ, s by the following:

$$\begin{cases} H(\theta, s) = H_{eq}(\theta) + s, \\ h(\theta, s) = h_{eq}(\theta) + s, \\ x(\theta, s) = x_{eq}(\theta) - 2s. \end{cases} \quad (4)$$

The transformation is well-defined for a 2-dimensional one-to-one mapping with an inverse function:

$$\begin{cases} \theta = \tan^{-1}\left(\frac{2h+x}{2H+x}\right), \\ s = Hh - \frac{x^2}{4}. \end{cases} \quad (5)$$

We could substitute this inverse transformation into the equilibrium solution Eq.(3) to obtain the equilibrium solution H_{eq}, h_{eq}, x_{eq} as the parameterizations of H, h, x :

$$\begin{cases} H_{eq} = \frac{1}{4}(2H+x)^2, \\ h_{eq} = \frac{1}{4}(2h+x)^2, \\ x_{eq} = \frac{1}{2}(2H+x)(2h+x). \end{cases} \quad (6)$$

This indicates two lessons. First, once we know the original set of genotype frequencies H, h, x as the initial condition, remarkably we can deduce the final equilibrium H_{eq}, h_{eq}, x_{eq} . Second, $(2H+x)$ and $(2h+x)$, these two numbers determine the final equilibrium. This implies, for the same number set of $(2H+x)$ and $(2h+x)$, even for different H, h, x , their final equilibriums are the same.

Substituting the reparameterization Eq.(4) to the governing equations Eq.(2), this not only decouples the parameters, but also decodes the equations to one time-dependent equation and the other time-independent equation:

$$\begin{cases} \frac{d}{dt}s = -k_b s, \\ \frac{d}{dt}\theta = 0. \end{cases} \quad (7)$$

Both are exactly solvable. Remarkably, **we have transformed the nonlinear coupled differential equations Eq.(2) to the linear decoupled differential equations Eq.(7).**

We foresee in advance the equilibrium solution is a global attractor, attracting all the points on the line direction of a certain given initial θ to the equilibrium point of the same θ in the exponential decay way along the s direction. Because each line direction for a θ is independent to each other with no intersection, this makes our solution well-defined everywhere in the parameter space. The global picture of time evolution is: giving any initial value in the parameter space, there is only one corresponding θ with a line direction of s connecting that equilibrium point to the initial value; the time evolution of parameters will go along the line direction to the equilibrium point in the exponential decay to reduce the distance away from the equilibrium point.

The method for deriving the analytic solution is the following: for any given initial value \tilde{H}, \tilde{h} and \tilde{x} , find the corresponding set of $\tilde{\theta}, \tilde{s}$. By Eq.(7), We then have $H(t)\tilde{H} + h(t)\tilde{h} + x(t)\tilde{x} = H_{eq}(\tilde{\theta})\tilde{H} + h_{eq}(\tilde{\theta})\tilde{h} + x_{eq}(\tilde{\theta})\tilde{x} + \tilde{s}e^{-k_b t}(\tilde{H} + \tilde{h} - 2\tilde{x})$. Because the transformation between old and new coordinate is well-defined, we can further solve the new equations and replace the parameters from θ, s to H, h, x by Eq.(5).

Hence, we achieve our exact analytic solution:

$$\begin{cases} H(t) = H_{eq}(\tan^{-1}(\frac{2\tilde{h}+\tilde{x}}{2\tilde{H}+\tilde{x}})) + (\tilde{H}\tilde{h} - \frac{\tilde{x}^2}{4})e^{-k_b t}, \\ h(t) = h_{eq}(\tan^{-1}(\frac{2\tilde{h}+\tilde{x}}{2\tilde{H}+\tilde{x}})) + (\tilde{H}\tilde{h} - \frac{\tilde{x}^2}{4})e^{-k_b t}, \\ x(t) = x_{eq}(\tan^{-1}(\frac{2\tilde{h}+\tilde{x}}{2\tilde{H}+\tilde{x}})) - 2(\tilde{H}\tilde{h} - \frac{\tilde{x}^2}{4})e^{-k_b t}. \end{cases} \quad (8)$$

The illustration of Eq.(8) is shown in Fig.3. The equilibrium solutions coincide with the De Finetti diagram [5].

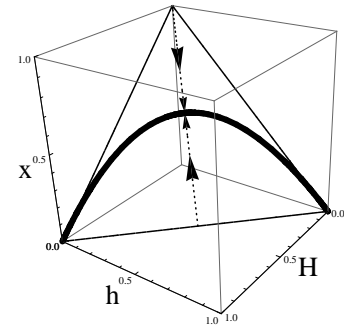


FIG. 3. The illustration of time-dependent exact analytic solutions Eq.(8) in the genotype frequency parameter space for the model of 2 alleles. The thick black curve stands for the 1-dimensional equilibrium solution Eq.(3). The dashed arrow direction indicates the 1-dimensional fiber direction $\hat{s} = \hat{H} + \hat{h} - 2\hat{x}$, where every point along the fiber line will be attracted to the thick black curve under time evolution.

Intuitively we would like to compare this model and its

analytic solution to experimental numerical data. It will be more appropriate to fit the experimental data into the equilibrium solution, because we can imagine that the genotype frequencies have been more-or-less stabilized within a closed population under the sufficient amount of time-evolution.

For this 1-Dominant-Gene-and-1-Recessive-Gene (hairstyle) model, the observables of available experimental data are the phenotypes, the representative biological characters, of curl (AA and Aa) and straight (aa) hairs. The two phenotype frequencies with one constraint, has 1 degree of freedom; this is the same as the 1 degree of freedom of the continuous equilibrium solution. The fitting can be perfectly with no error bar; however, this is due to the same degree of freedom of correspondence, rather than the evidence of successful description of this model. Hence, the hairstyle experimental data cannot illustrate the validity of the theory.

In the next, we shall turn to the next-simplest model: 3 alleles, such as 2 dominant genes and 1 recessive gene case, for example, the blood-type model, to check the experimental evidence of our theory.

B. Model of 3 Alleles: 2 Dominant Genes and 1 Recessive Gene: Blood Type Evolution Model

1. Governing equations and exact analytic solutions

For the model of 3 alleles, such as two dominant genes A , B and one recessive gene i of blood types, the representative phenotypes are type A: AA and Ai , type B: BB and Bi , type AB: AB , and type O: ii .

$$\left\{ \begin{array}{l} \text{Type O: } o \text{ represents } ii, \\ \text{Type A: } a \text{ represents } AA, \\ \quad \quad x \text{ represents } Ai, \\ \text{Type B: } b \text{ represents } BB, \\ \quad \quad y \text{ represents } Bi, \\ \text{Type AB: } c \text{ represents } AB. \end{array} \right.$$

There are four kinds of representative phenotypes (A, B, AB, O), and six parameters of genotype population (o, a, b, x, y, c), for a total population $o+a+b+x+y+c = P$. Here we follow the similar derivation as the previous model in Sec III A. to write down the governing equations for the *population parameters*:

$$\left\{ \begin{array}{l} \frac{do}{dt} = k_b \frac{1}{P} (o^2 + ox + oy + \frac{x^2}{4} + \frac{y^2}{4} + \frac{xy}{2}) - k_d o, \\ \frac{da}{dt} = k_b \frac{1}{P} (a^2 + ac + ax + \frac{c^2}{4} + \frac{x^2}{4} + \frac{cx}{2}) - k_d a, \\ \frac{db}{dt} = k_b \frac{1}{P} (b^2 + by + bc + \frac{y^2}{4} + \frac{c^2}{4} + \frac{yc}{2}) - k_d b, \\ \frac{dx}{dt} = k_b \frac{1}{P} (2oa + ox + ax + oc + ay + \frac{xy}{2} + \frac{xc}{2} + \frac{yc}{2} + \frac{x^2}{2}) - k_d x, \\ \frac{dy}{dt} = k_b \frac{1}{P} (2ob + by + oy + bx + oc + \frac{yc}{2} + \frac{yx}{2} + \frac{cx}{2} + \frac{y^2}{2}) - k_d y, \\ \frac{dc}{dt} = k_b \frac{1}{P} (2ab + ac + bc + ay + bx + \frac{cx}{2} + \frac{cy}{2} + \frac{xy}{2} + \frac{c^2}{2}) - k_d c. \end{array} \right. \quad (9)$$

By redefining $\frac{G}{P} \rightarrow G$ as the *percentage parameters*, where G is any of the six parameters, we can derive the

governing *percentage parameters* equations for *genotype frequencies*:

$$\left\{ \begin{array}{l} \frac{do}{dt} = k_b (o^2 + ox + oy + \frac{x^2}{4} + \frac{y^2}{4} + \frac{xy}{2} - o), \\ \frac{da}{dt} = k_b (a^2 + ac + ax + \frac{c^2}{4} + \frac{x^2}{4} + \frac{cx}{2} - a), \\ \frac{db}{dt} = k_b (b^2 + by + bc + \frac{y^2}{4} + \frac{c^2}{4} + \frac{yc}{2} - b), \\ \frac{dx}{dt} = k_b (2oa + ox + ax + oc + ay + \frac{xy}{2} + \frac{xc}{2} + \frac{yc}{2} + \frac{x^2}{2} - x), \\ \frac{dy}{dt} = k_b (2ob + by + oy + bx + oc + \frac{yc}{2} + \frac{yx}{2} + \frac{cx}{2} + \frac{y^2}{2} - y), \\ \frac{dc}{dt} = k_b (2ab + ac + bc + ay + bx + \frac{cx}{2} + \frac{cy}{2} + \frac{xy}{2} + \frac{c^2}{2} - c). \end{array} \right. \quad (10)$$

Now, we generalize the equilibrium solution (3) of Eq.(2) to the equilibrium solution of Eq.(10):

$$\left\{ \begin{array}{l} o_{eq}(\theta_1, \theta_2) = \frac{\cos^2(\theta_1)}{(\cos(\theta_1)+\sin(\theta_1))^2}, \\ a_{eq}(\theta_1, \theta_2) = \frac{\sin^2(\theta_1)}{(\cos(\theta_1)+\sin(\theta_1))^2} \frac{\cos^2(\theta_2)}{(\cos(\theta_2)+\sin(\theta_2))^2}, \\ b_{eq}(\theta_1, \theta_2) = \frac{\sin^2(\theta_1)}{(\cos(\theta_1)+\sin(\theta_1))^2} \frac{\sin^2(\theta_2)}{(\cos(\theta_2)+\sin(\theta_2))^2}, \\ x_{eq}(\theta_1, \theta_2) = \frac{2 \sin(\theta_1) \cos(\theta_1)}{(\cos(\theta_1)+\sin(\theta_1))^2} \frac{\cos(\theta_2)}{\cos(\theta_2)+\sin(\theta_2)}, \\ y_{eq}(\theta_1, \theta_2) = \frac{2 \sin(\theta_1) \cos(\theta_1)}{(\cos(\theta_1)+\sin(\theta_1))^2} \frac{\sin(\theta_2)}{\cos(\theta_2)+\sin(\theta_2)}, \\ c_{eq}(\theta_1, \theta_2) = \frac{\sin^2(\theta_1)}{(\cos(\theta_1)+\sin(\theta_1))^2} \frac{2 \sin(\theta_2) \cos(\theta_2)}{(\cos(\theta_2)+\sin(\theta_2))^2}. \end{array} \right. \quad (11)$$

We can further make the above 2-dimensional equilibrium parameterization an one-to-one mapping to (θ_1, θ_2) , if we define that $\theta_1 = 0, \forall \theta_2$ shrinks into a point. Namely, (θ_1, θ_2) can be a well-defined one-to-one reparameterization of the equilibrium solution Eq.(11).

The linear stability analysis shows this system is again locally stable with five eigenvalues $0, 0, -1, -1, -1$ [14]. Here two 0 eigenvalues correspond to two eigenvectors along the *marginal* tangent plane [14] of 2-dimensional equilibrium solutions, three -1 eigenvalues correspond to the *stable perturbation* [14] along the three eigenvectors $\hat{o} + \hat{a} - 2\hat{x}$, $\hat{o} + \hat{b} - 2\hat{y}$, $\hat{a} + \hat{b} - 2\hat{c}$. Defining those eigenvectors as $\hat{s}_{01}, \hat{s}_{02}, \hat{s}_{12}$ with coordinates s_{01}, s_{02}, s_{12} , we could transform (o, a, b, x, y, c) of the whole parameter space (6-dimensions with 1 constraint $o+a+b+x+y+c=1$) to a set of 5-dimensional new coordinates $(\theta_1, \theta_2, s_{01}, s_{02}, s_{12})$:

$$\left\{ \begin{array}{l} o = o_{eq}(\theta_1, \theta_2) + s_{01} + s_{02}, \\ a = a_{eq}(\theta_1, \theta_2) + s_{01} + s_{12}, \\ b = b_{eq}(\theta_1, \theta_2) + s_{02} + s_{12}, \\ x = x_{eq}(\theta_1, \theta_2) - 2s_{01}, \\ y = y_{eq}(\theta_1, \theta_2) - 2s_{02}, \\ c = c_{eq}(\theta_1, \theta_2) - 2s_{12}. \end{array} \right. \quad (12)$$

We have the following inverse function:

$$\left\{ \begin{array}{l} \theta_1 = \tan^{-1} \left(\frac{2(a+b+c)+x+y}{2o+x+y} \right), \\ \theta_2 = \tan^{-1} \left(\frac{2b+y+c}{2a+x+c} \right), \\ s_{01} = ao + \frac{ay}{2} + \frac{oc}{2} - \frac{xb}{2} - \frac{xc}{4} - \frac{xy}{4} - \frac{x^2}{4} + \frac{cy}{4}, \\ s_{02} = ba + \frac{bx}{2} + \frac{ay}{2} - \frac{co}{2} - \frac{cy}{4} - \frac{cx}{4} - \frac{c^2}{4} + \frac{yx}{4}, \\ s_{12} = ob + \frac{oc}{2} + \frac{bx}{2} - \frac{ya}{2} - \frac{yx}{4} - \frac{yc}{4} - \frac{y^2}{4} + \frac{xc}{4}. \end{array} \right. \quad (13)$$

Substitute the reparameterization Eq.(12) to Eq.(10), we confirm again this system will be global stable like the previous model in Sec.III A.

2. Experimental evidence - data fitting

$$\begin{cases} \frac{d}{dt}s_{01} = -k_b s_{01}, \\ \frac{d}{dt}s_{02} = -k_b s_{02}, \\ \frac{d}{dt}s_{12} = -k_b s_{12}, \\ \frac{d}{dt}\theta_1 = 0, \\ \frac{d}{dt}\theta_2 = 0. \end{cases} \quad (14)$$

The analytic solution is determined by a given set of initial values $\tilde{o}, \tilde{a}, \tilde{b}, \tilde{x}, \tilde{y}, \tilde{c}$, which correspond to a set of $\tilde{\theta}_1, \tilde{\theta}_2, \tilde{s}_{01}, \tilde{s}_{02}, \tilde{s}_{12}$ via Eq.(13). We obtain the exact analytic time-dependent dynamical solution:

$$\begin{cases} o(t) = o_{eq}(\tilde{\theta}_1, \tilde{\theta}_2) + \tilde{s}_{01}e^{-k_b t} + \tilde{s}_{02}e^{-k_b t}, \\ a(t) = a_{eq}(\tilde{\theta}_1, \tilde{\theta}_2) + \tilde{s}_{01}e^{-k_b t} + \tilde{s}_{12}e^{-k_b t}, \\ b(t) = b_{eq}(\tilde{\theta}_1, \tilde{\theta}_2) + \tilde{s}_{02}e^{-k_b t} + \tilde{s}_{12}e^{-k_b t}, \\ x(t) = x_{eq}(\tilde{\theta}_1, \tilde{\theta}_2) - 2\tilde{s}_{01}e^{-k_b t}, \\ y(t) = y_{eq}(\tilde{\theta}_1, \tilde{\theta}_2) - 2\tilde{s}_{02}e^{-k_b t}, \\ c(t) = c_{eq}(\tilde{\theta}_1, \tilde{\theta}_2) - 2\tilde{s}_{12}e^{-k_b t}. \end{cases} \quad (15)$$

The illustration of Eq.(15) is shown in Fig.4.

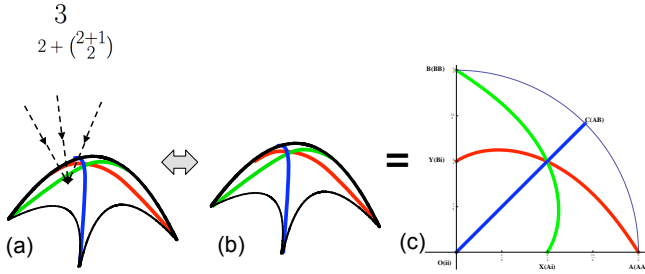


FIG. 4. (a) The illustration of time-dependent exact analytic solutions Eq.(15), solved from Eq.(10), in the genotype frequency parameter space for the model of 3 alleles. The surface stands for the 2-dimensional equilibrium solution Eq.(11). The dashed arrows indicate the 3-dimensional fiber spanned by 3 vectors: $\hat{s}_{01} = \hat{o} + \hat{a} - 2\hat{x}$, $\hat{s}_{02} = \hat{o} + \hat{b} - 2\hat{y}$ and $\hat{s}_{12} = \hat{a} + \hat{b} - 2\hat{c}$, where every point along the 3-dimensional fibers will be attracted to the 2-dimensional stable equilibrium manifold Eq.(11) under time evolution. (b) The illustration of 2-dimensional stable equilibrium manifold Eq.(11), which is mapped to (c) the 2-dimensional quadrant $(\theta_1 \cos(\theta_2), \theta_1 \sin(\theta_2))$ parametrized by (θ_1, θ_2) , detailed shown in FIG.5.

The dimensionality: We shall explain the physical meaning on the dimensionality of the fibers and the stable base manifold. For both Eq.(9) and Eq.(10), there is a permutation symmetric group S_3 symmetry by exchanging A, B, i and their corresponding genotypes. The S_3 symmetry also results in time-independent *conserved quantities*, spanned by $o+a-2x$, $o+b-2y$ and $a+b-2c$, with a constraint $o+a+b+x+y+c=1$. There are totally 2 independent degrees of freedom. We can say the S_3 symmetry results in the dimensionality of fixed-point solutions is 2, here parametrized by θ_1, θ_2 .

As we mentioned, we would like to fit the available blood type data - blood type population percentages as *genotype frequencies* of any ethnic group, into our equilibrium solutions on the stable 2-dimensional manifold of Eq.(11). For a set of genotype frequencies (ii, AA, BB, Ai, Bi, AB) , it totally forms a set of 5-dimensional degrees of freedom (due to 6 numbers with 1 constraint). We could correlate this with $(o(\theta_1, \theta_2), a(\theta_1, \theta_2), b(\theta_1, \theta_2), x(\theta_1, \theta_2), y(\theta_1, \theta_2), c(\theta_1, \theta_2))$ for a 2-dimensional parameterization (θ_1, θ_2) . In this way, there would be a correspondence between 5-dimensions and 2-dimensions, the validity of experimental fitness to our theoretical (θ_1, θ_2) prediction would be a strong evidence for the validity of our model. However, current available experimental data we found is just $(O_{exp}, A_{exp}, B_{exp}, AB_{exp})$, which is 3-dimensional (4 numbers with 1 constraint) $(ii, AA + Ai, BB + Bi, AB)$; we would then correlate this to $(o(\theta_1, \theta_2), a(\theta_1, \theta_2) + x(\theta_1, \theta_2), b(\theta_1, \theta_2) + y(\theta_1, \theta_2), c(\theta_1, \theta_2))$ for certain 2-dimensional parameters (θ_1, θ_2) . The test for the validity of this theory now becomes a correspondence between 3-dimensions to 2-dimensions. We fit the 3-dimensional experimental data into our 2-dimensional equilibrium solutions. Although this is not as stringent as the 5-dimensional to 2-dimensional correspondence, there remains one degree of freedom for experimental data to deviate from our equilibrium solution. If the error bar for this 3-dimensional to 2-dimensional correspondence is tiny, then our theory shows consistency to the level of predicting the stability of genotype frequencies.

Our fitting procedure is to solve (θ_1, θ_2) from two equalities:

$$\begin{cases} A_{exp} = a(\theta_1, \theta_2) + x(\theta_1, \theta_2), \\ B_{exp} = b(\theta_1, \theta_2) + y(\theta_1, \theta_2). \end{cases} \quad (16)$$

Then, with applicable $(\tilde{\theta}_1, \tilde{\theta}_2)$ as solutions of equalities, we can further know $o(\tilde{\theta}_1, \tilde{\theta}_2) \equiv O_t$ and $c(\tilde{\theta}_1, \tilde{\theta}_2) \equiv AB_t$. Since $A_{exp} = A_t$ and $B_{exp} = B_t$ by Eq.(16), we could test the differences and error bars of O and AB as follows:

$$\begin{cases} O_t - O_{exp} \equiv \text{Diff}\%(O_t - O_{exp}), \\ AB_t - AB_{exp} \equiv \text{Diff}\%(AB_t - AB_{exp}), \\ \frac{O_t - O_{exp}}{O_{exp}} \equiv \text{Error}\%(\frac{O_t - O_{exp}}{O_{exp}}), \\ \frac{AB_t - AB_{exp}}{AB_{exp}} \equiv \text{Error}\%(\frac{AB_t - AB_{exp}}{AB_{exp}}). \end{cases} \quad (17)$$

As we mention the 2-dimensional equilibrium parameterization is an one-to-one mapping if we define that $\theta_1 = 0, \forall \theta_2$ shrinks into a point. Hence, we can introduce the $(\theta_1 \cos(\theta_2), \theta_1 \sin(\theta_2))$ polar coordinates mapped from the Eq.(11) of the parameter (θ_1, θ_2) . In other words, we define that θ_1 represents the radial direction $(0 \leq \theta_1 \leq \frac{\pi}{2})$, θ_2 represents the angle direction $(0 \leq \theta_2 \leq \frac{\pi}{2})$ for our

stable equilibrium solution diagram, show in FIG.5 as our blood type mapping *chart*. This chart is a quadrant: one fourth of a circle. Inside the quadrant consists of all stable fixed points mapping from the 2-dimensional manifold Eq.(11). At three corners of the quadrant, there are $o \equiv O(ii)$, $a \equiv A(AA)$, and $b \equiv B(BB)$. For specifying their Cartesian coordinates (o, a, b, x, y, c) , each of these is 100% of that specified type - e.g. $O(ii) = (1, 0, 0, 0, 0, 0)$, $A(AA) = (0, 1, 0, 0, 0, 0)$, $B(BB) = (0, 0, 1, 0, 0, 0)$. Similarly, at the midpoints of the three edge sides, we have $X(Ai) = (\frac{1}{2}, \frac{1}{4}, 0, \frac{1}{2}, 0, 0)$, $Y(Bi) = (\frac{1}{2}, 0, \frac{1}{4}, 0, \frac{1}{2}, 0)$, and $C(AB) = (0, 0, 0, \frac{1}{4}, \frac{1}{4}, \frac{1}{2})$. The blue line represents the symmetric line invariant under switching a, x to b, y .

From Eq.(11), we could easily see the blue line is $\theta_2 = \frac{\pi}{4}$. The green curve represents the symmetry invariant under switching a, c to o, y . This gives the green curve parameterization:

$$\theta_1(\theta_2) = \frac{(\sqrt{3 + \cos(2\theta_2)} + 2\sin(2\theta_2))(1 + \tan(\theta_2))}{\sqrt{2 + 2\sin(2\theta_2)}}. \quad (18)$$

The red curve represents the symmetry invariant under switching b, c to o, x . This gives the red curve parameterization:

$$\theta_1(\theta_2) = \frac{(\sqrt{3 - \cos(2\theta_2)} + 2\sin(2\theta_2))(1 + \cot(\theta_2))}{\sqrt{2 + 2\sin(2\theta_2)}}. \quad (19)$$

The intersection of three color lines, is $(\frac{2}{9}, \frac{2}{9}, \frac{2}{9}, \frac{1}{9}, \frac{1}{9}, \frac{1}{9})$, which is the most symmetric mid point.

3. Explanation and application of the chart - relations of different ethnic groups by geodesic distances

The experimental data that we implemented is mainly from two data resources [13]. We fit the experimental data [13] for both (1) different ethnic groups and (2) different countries. We present the **experimental data** ($O_{exp}, A_{exp}, B_{exp}, AB_{exp}$) in Table.I, III, IV. We present our corresponding **theoretical prediction**, the data ($O_t, AA_t, Ai_t, BB_t, Bi_t, AB_t$) in Table.II, V, VI.

Data fitting for ethnic groups is much promising, because random mating assumption is approximately true for a certain given ethnic group. On the other hand, a country may possess multi-ethnicities where the random mating assumption generally fails for the country with multi-ethnic groups.

We also investigate the data distribution of different ethnic groups and countries under our (θ_1, θ_2) domain space. We found some facts:

- (1) American aboriginals possess large portion of Type O.
- (2) Europeans or Caucasians possess much more Type A than others.
- (3) Mongolians, like Buryats, possess comparably more

Type B.

(4) Diff% and Error% for islanders, like Irish and Japanese, are smaller than races living in a larger continent, like Hindus. Thus, we can say that the closed system assumption plays an important rule such that the data of islanders are more close to the stable fixed-point equilibrium solutions.

In our plots (see Figures in Sec.VIII), θ_1 represents the radial direction ($0 \leq \theta_1 \leq \frac{\pi}{2}$), θ_2 represents the angle direction ($0 \leq \theta_2 \leq \frac{\pi}{2}$). We invent the *chart* to organize the data - for the blood type model, we have a *quadrant* spanned by θ_1 and θ_2 with the horizontal and vertical coordinates as $(\theta_1 \cos(\theta_2), \theta_1 \sin(\theta_2))$. We propose the distribution of different ethnic groups (marked with numbers) in our plots would reveal their relative distance correlations. More precisely, **to quantitatively define the distance between two ethnic groups, we propose a mathematical method to achieve this by solving the geodesic equation** numerically from the given metric of stable-solution manifold.

For the model of 2 alleles studied here in Sec.III A, we can write down the intrinsic metric of 1-dimensional equilibrium manifold Eq.(3). This can be done by considering the infinitesimal distance ds in the genotype frequency space by transforming the Euclidean (H, h, x) space to the curved space (θ_1) :

$$\begin{aligned} ds^2 &= dH^2 + dh^2 + dx^2 = \left(\left(\frac{\partial H}{\partial \theta_1}\right)^2 + \left(\frac{\partial h}{\partial \theta_1}\right)^2 + \left(\frac{\partial x}{\partial \theta_1}\right)^2\right) d\theta_1^2 \\ &\equiv g_{\theta_1, \theta_1} d\theta_1^2 \end{aligned} \quad (20)$$

For example, for the model of 3 alleles studied in Sec.III B, we can write down the intrinsic metric of 2-dimensional equilibrium manifold Eq.(11). This can be done by considering the infinitesimal distance ds in the genotype frequency space by transforming the Euclidean (o, a, b, x, y, c) space to the curved space (θ_1, θ_2) :

$$\begin{aligned} ds^2 &= do^2 + da^2 + db^2 + dx^2 + dy^2 + dc^2 \\ &\equiv g_{\theta_1, \theta_1} d\theta_1^2 + 2g_{\theta_1, \theta_2} d\theta_1 d\theta_2 + g_{\theta_2, \theta_2} d\theta_2^2 = g_{\mu\nu} d\theta_\mu d\theta_\nu, \end{aligned} \quad (21)$$

where in the second line all the parameters are re-written in terms of (θ_1, θ_2) , e.g. $do = (\frac{\partial o}{\partial \theta_1}) d\theta_1 + (\frac{\partial o}{\partial \theta_2}) d\theta_2$, etc. We propose that:

The genetic distance between two ethnic groups with stabilized genotype frequencies can be defined as the geodesic length by solving the geodesic equation on the stable equilibrium manifold.

On one hand, we could further define this least distance as the “genetic distance” between any pair of two ethnic groups. On the other hand, by comparing the geographical distribution of ethnic groups and the distribution of ethnic groups on our equilibrium-solution chart, we find their strong correlation and certain meaningful pattern. The details of the data of geodesic distance shall be left for the future.

Index	Ethnic (People Group)	$O_{exp}(\%)$	$A_{exp}(\%)$	$B_{exp}(\%)$	$AB_{exp}(\%)$	θ_1	θ_2	Diff%(O_t-O_{exp})	Diff%(AB_t-AB_{exp})
1	Aborigines	61	39	0	0	0.2734	0.0000	0.0000	0.0000
2	Abyssinians	43	27	25	5	0.5011	0.7511	-1.2547	1.2547
3	Albanians	38	43	13	6	0.5487	0.3314	0.5169	-0.5169
4	Arabs	34	31	29	6	0.6971	0.7570	-4.3754	4.3754
5	Armenians	31	50	13	6	0.7012	0.3027	-1.6005	1.6005
6	Asian(USA)	40	28	27	5	0.5646	0.7694	-2.5159	2.5159
7	Bantus	46	30	19	5	0.4423	0.5843	0.0498	-0.0498
8	Basques	51	44	4	1	0.3860	0.1052	-0.4424	0.4424
9	Belgians	47	42	8	3	0.4285	0.2140	0.1153	-0.1153
10	Blackfoot(N. Am. Indian)	17	82	0	1	0.9357	0.0000	1.0000	-1.0000
11	Bororo	100	0	0	0	0.0000		0.0000	0.0000
12	Brazilians	47	41	9	3	0.4323	0.2437	-0.1799	0.1799
13	Burmese	36	24	33	7	0.6087	0.9224	-1.2738	1.2738
14	Buryats	33	21	38	8	0.6504	1.0313	-0.7470	0.7470
15	Chinese-Canton	46	23	25	6	0.4290	0.8232	1.0825	-1.0825
16	Danes	41	44	11	4	0.5206	0.2798	-0.6050	0.6050
17	Dutch	45	43	9	3	0.4622	0.2354	-0.4505	0.4505
18	Eskimos(Alaska)	38	44	13	5	0.5680	0.3264	-0.7347	0.7347
19	Finns	34	41	18	7	0.6372	0.4546	-0.9803	0.9803
20	French	43	47	7	3	0.4836	0.1736	-0.0098	0.0098
21	Germans	41	43	11	5	0.5034	0.2842	0.5868	-0.5868
22	Hindus(Bombay)	32	29	28	11	0.6127	0.7701	2.4826	-2.4826
23	Hungarians	36	43	16	5	0.6267	0.3990	-2.3598	2.3598
24	Indians(USA)	79	16	4	1	0.1201	0.2532	0.6212	-0.6212
25	Irish	52	35	10	3	0.3667	0.3035	0.2035	-0.2035
26	Japanese	30	38	22	10	0.6810	0.5591	0.5134	-0.5134
27	Jews(Germany)	42	41	12	5	0.4907	0.3184	0.4772	-0.4772
28	Jews(Poland)	33	41	18	8	0.6372	0.4546	0.0197	-0.0197
29	Kikuyu(Kenya)	60	19	20	1	0.3015	0.8093	-1.8112	1.8112
30	Lapps	29	63	4	4	0.6892	0.0847	1.0566	-1.0566
31	Latvians	32	37	24	7	0.7180	0.6056	-3.5096	3.5096
32	Lithuanians	40	34	20	6	0.5345	0.5582	-0.5444	0.5444
33	Malasians	62	18	20	0	0.2894	0.8346	-2.6261	2.6261
34	Moros	64	16	20	0	0.2663	0.8895	-2.2717	2.2717
35	Navajo(N. Am. Indain)	73	27	0	0	0.1688	0.0000	0.0000	0.0000
36	Papuas(New Guinea)	41	27	23	9	0.4631	0.7135	3.4828	-3.4828
37	Persians	38	33	22	7	0.5594	0.6103	-0.1801	0.1801
38	Peru(Indians)	100	0	0	0	0.0000		0.0000	0.0000
39	Philippinos	45	22	27	6	0.4452	0.8774	0.8265	-0.8265
40	Portuguese	35	53	8	4	0.6123	0.1834	-0.4928	0.4928
41	Rumanians	34	41	19	6	0.6673	0.4755	-2.7138	2.7138
42	Russians	33	36	23	8	0.6572	0.5969	-1.1401	1.1401
43	Sardinians	50	26	19	5	0.3808	0.6435	0.9971	-0.9971
44	Scotts	51	34	12	3	0.3846	0.3659	-0.3254	0.3254
45	Shompen(Nicobars)	100	0	0	0	0.0000		0.0000	0.0000
46	Slovaks	42	37	16	5	0.5049	0.4409	-0.5190	0.5190
47	South Africans	45	40	11	4	0.4547	0.2993	0.1149	-0.1149
48	Spanish	38	47	10	5	0.5510	0.2447	0.3680	-0.3680
49	Swedes	38	47	10	5	0.5510	0.2447	0.3680	-0.3680
50	Swiss	40	50	7	3	0.5321	0.1666	-0.3848	0.3849
51	Tartars	28	30	29	13	0.6671	0.7708	3.2975	-3.2975
52	Thais	37	22	33	8	0.5594	0.9605	0.8199	-0.8199
53	United Kingdom(GB)	47	42	8	3	0.4285	0.2140	0.1153	-0.1153
54	USA(blacks)	49	27	20	4	0.4114	0.6504	-0.5293	0.5293
55	USA(whites)	45	40	11	4	0.4547	0.2993	0.1149	-0.1149

TABLE I. ETHNIC GROUP.1 This table shows available **experimental data** of blood type ratios of O,A,B, and AB (denoted with a sub-indices “exp.”) for 55 different ethnics (ethnic groups) around the world [13]. The index of certain ethnic corresponds to the specified number of a data point distributed on the plots of FIG 6, FIG 7, FIG 14 and FIG 15. We fit blood type population percentage of available experimental results to the 2 parameter spaces θ_1 and θ_2 of our equilibrium solution. The error bar is comparably small. The FIG 6, 7, 14 and 15 (the mappings of equilibrium solutions) may be a good way of data organization for revealing the relations of different ethnic groups.

Index	Ethnic (People Group)	$O_t(\%)$	$AA_t(\%)$	$Ai_t(\%)$	$BB_t(\%)$	$Bi_t(\%)$	$AB_t(\%)$	Error%($\frac{O_t - O_{exp}}{O_{exp}}$)	Error%($\frac{AB_t - AB_{exp}}{AB_{exp}}$)
1	Aborigines	61.00	4.80	34.21	0.00	0.00	0.00	0.00	
2	Abyssinians	41.75	3.35	23.65	2.92	22.08	6.25	-2.92	25.09
3	Albanians	38.52	7.97	35.03	0.94	12.06	5.48	1.36	-8.62
4	Arabs	29.62	5.49	25.51	4.90	24.10	10.38	-12.87	72.92
5	Armenians	29.40	12.17	37.83	1.19	11.81	7.60	-5.16	26.67
6	Asian(USA)	37.48	3.88	24.12	3.64	23.36	7.52	-6.29	50.32
7	Bantus	46.05	3.74	26.26	1.64	17.36	4.95	0.11	-1.00
8	Basques	50.56	6.83	37.17	0.08	3.92	1.44	-0.87	44.24
9	Belgians	47.12	6.64	35.36	0.31	7.69	2.88	0.25	-3.84
10	Blackfoot(N. Am. Indian)	18.00	33.15	48.85	0.00	0.00	0.00	5.88	-100.00
11	Bororo	100.00	0.00	0.00	0.00	0.00	0.00	0.00	
12	Brazilians	46.82	6.39	34.61	0.40	8.60	3.18	-0.38	6.00
13	Burmese	34.73	3.13	20.87	5.46	27.54	8.27	-3.54	18.20
14	Buryats	32.25	2.62	18.38	7.30	30.70	8.75	-2.26	9.34
15	Chinese-Canton	47.08	2.28	20.72	2.65	22.35	4.92	2.35	-18.04
16	Danes	40.40	8.01	35.99	0.66	10.34	4.60	-1.48	15.12
17	Dutch	44.55	7.19	35.81	0.41	8.59	3.45	-1.00	15.02
18	Eskimos(Alaska)	37.27	8.47	35.53	0.97	12.03	5.73	-1.93	14.69
19	Finns	33.02	8.16	32.84	1.95	16.05	7.98	-2.88	14.00
20	French	42.99	8.58	38.42	0.26	6.74	3.01	-0.02	0.33
21	Germans	41.59	7.55	35.45	0.64	10.36	4.41	1.43	-11.74
22	Hindus(Bombay)	34.48	4.39	24.61	4.13	23.87	8.52	7.76	-22.57
23	Hungarians	33.64	8.73	34.27	1.55	14.45	7.36	-6.56	47.20
24	Indians(USA)	79.62	0.73	15.27	0.05	3.95	0.38	0.79	-62.12
25	Irish	52.20	4.47	30.53	0.44	9.56	2.80	0.39	-6.78
26	Japanese	30.51	7.58	30.42	2.97	19.03	9.49	1.71	-5.13
27	Jews(Germany)	42.48	6.86	34.14	0.75	11.25	4.52	1.14	-9.54
28	Jews(Poland)	33.02	8.16	32.84	1.95	16.05	7.98	0.06	-0.25
29	Kikuyu(Kenya)	58.19	1.34	17.66	1.47	18.53	2.81	-3.02	181.12
30	Lapps	30.06	17.34	45.66	0.12	3.88	2.94	3.64	-26.42
31	Latvians	28.49	7.59	29.41	3.64	20.36	10.51	-10.97	50.14
32	Lithuanians	39.46	5.24	28.76	2.04	17.96	6.54	-1.36	9.07
33	Malasians	59.37	1.19	16.81	1.45	18.55	2.63	-4.24	
34	Moros	61.73	0.92	15.08	1.40	18.60	2.27	-3.55	
35	Navajo(N. Am. Indain)	73.00	2.12	24.88	0.00	0.00	0.00	0.00	
36	Papuas(New Guinea)	44.48	3.19	23.81	2.39	20.61	5.52	8.49	-38.70
37	Persians	37.82	5.13	27.87	2.51	19.49	7.18	-0.47	2.57
38	Peru(Indians)	100.00	0.00	0.00	0.00	0.00	0.00	0.00	
39	Philippinos	45.83	2.15	19.85	3.11	23.89	5.17	1.84	-13.77
40	Portuguese	34.51	12.11	40.89	0.42	7.58	4.49	-1.41	12.32
41	Rumanians	31.29	8.46	32.54	2.24	16.76	8.71	-7.98	45.23
42	Russians	31.86	6.72	29.28	3.11	19.89	9.14	-3.45	14.25
43	Sardinians	51.00	2.67	23.33	1.50	17.50	4.00	1.99	-19.94
44	Scotts	50.67	4.34	29.66	0.64	11.36	3.33	-0.64	10.85
45	Shompen(Nicobars)	100.00	0.00	0.00	0.00	0.00	0.00	0.00	
46	Slovaks	41.48	5.85	31.15	1.30	14.70	5.52	-1.24	10.38
47	South Africans	45.11	6.30	33.70	0.60	10.40	3.89	0.26	-2.87
48	Spanish	38.37	9.27	37.73	0.58	9.42	4.63	0.97	-7.36
49	Swedes	38.37	9.27	37.73	0.58	9.42	4.63	0.97	-7.36
50	Swiss	39.62	10.06	39.94	0.28	6.72	3.38	-0.96	12.83
51	Tartars	31.30	4.99	25.01	4.71	24.29	9.70	11.78	-25.37
52	Thais	37.82	2.51	19.49	5.13	27.87	7.18	2.22	-10.25
53	United Kingdom(GB)	47.12	6.64	35.36	0.31	7.69	2.88	0.25	-3.84
54	USA(blacks)	48.47	2.98	24.02	1.72	18.28	4.53	-1.08	13.23
55	USA(whites)	45.11	6.30	33.70	0.60	10.40	3.89	0.26	-2.87

TABLE II. ETHNIC GROUP.2 This table continues from the previous TABLE I. This TABLE II shows our **theoretical prediction** corresponding to the experimental data of TABLE I. The experiment data fitting procedure is that we use two constraints type A (AA and Ai) and type B (BB and Bi), comparing these with 2-dimensional equilibrium solution, and finding out total 6 different blood types by our **theoretical stable fixed-point prediction**. In this table, we compute the error bar of O and AB. In addition, we compute our theoretical prediction on the population ratio of AA and Ai , BB and Bi . For the usual blood type test, these data may not be easily determined. However, we compile our theoretical prediction data here which may be testable data for future experiments.

Index	Country	$O_{exp}(\%)$	$A_{exp}(\%)$	$B_{exp}(\%)$	$AB_{exp}(\%)$	θ_1	θ_2	Diff%($O_t - O_{exp}$)	Diff%($AB_t - AB_{exp}$)
1	Canada	41	45	10	4	0.5156	0.2519	-0.2600	0.2600
2	USA	45	41	10	4	0.4510	0.2691	0.3930	-0.3930
3	Mexico	84	11	4	1	0.0860	0.3550	0.7512	-0.7512
4	Guatemala	95	3	2	0	0.0261	0.5892	-0.0312	0.0312
5	El Salvador	60	26	11	3	0.2738	0.4187	0.9503	-0.9503
6	Nicaragua	92	7	1	0	0.2738	0.1441	-0.0373	0.0373
7	Costa Rica	53	31	13	3	0.3597	0.4210	-0.1914	0.1914
8	Cuba	49	36	12	3	0.4128	0.3503	-0.6358	0.6358
9	Jamaica	56	20	21	3	0.3266	0.8080	-0.1988	0.1988
10	Dominican Rep	53	31	13	3	0.3597	0.4210	-0.1914	0.1914
11	Haiti	51	27	18	4	0.3800	0.6035	0.0651	-0.0651
12	Puerto Rico	47	30	13	10	0.3468	0.4317	6.9573	-6.9573
13	Colombia	62	27	9	2	0.2610	0.3401	0.2843	-0.2843
14	Ecuador	63	29	6	2	0.2469	0.2195	0.7914	-0.7914
15	Peru	71	19	9	1	0.1855	0.4544	-0.1006	0.1006
16	Chile	56	31	10	3	0.3174	0.3342	0.6607	-0.6607
17	Bolivia	93	5	2	0	0.0372	0.3832	-0.0528	0.0528
18	Venezuela	44	37	14	5	0.4645	0.3933	0.3814	-0.3814
19	Brazil	48	39	10	3	0.4213	0.2793	-0.3173	0.3173
20	Argentina	48	39	10	3	0.4213	0.2793	-0.3173	0.3173
21	Paraguay	56	34	9	1	0.3393	0.2818	-1.3696	1.3696
22	Uruguay	45	42	10	3	0.4664	0.2644	-0.7603	0.7603
23	Australia	47	40	10	3	0.4359	0.2740	-0.4594	0.4594
24	New Zealand	48	40	9	3	0.4180	0.2483	-0.0520	0.0520
25	Iceland	56	32	10	2	0.3293	0.3258	-0.4484	0.4484
26	Ireland	54	33	10	3	0.3414	0.3179	0.4391	-0.4391
27	United Kingdom	47	41	9	3	0.4323	0.2437	-0.1799	0.1799
28	Scotland	51	35	11	3	0.3823	0.3310	-0.1307	0.1307
29	England	46	43	8	3	0.4430	0.2103	-0.0025	0.0025
30	Norway	39	49	8	4	0.5386	0.1922	0.1844	-0.1844
31	Sweden	38	47	10	5	0.5510	0.2447	0.3680	-0.3680
32	Finland	33	42	18	7	0.6619	0.4480	-1.4095	1.4095
33	Denmark	42	44	10	4	0.4987	0.2558	-0.0863	0.0863
34	Netherlands	45	43	9	3	0.4622	0.2354	-0.4505	0.4505
35	Belgium	46	43	8	3	0.4430	0.2103	-0.0025	0.0025
36	France	43	45	9	3	0.4938	0.2279	-0.7431	0.7431
37	Spain	42	45	9	4	0.4938	0.2279	0.2569	-0.2569
38	Portugal	41	48	8	3	0.5215	0.1948	-0.6655	0.6655
39	Germany	38	43	13	6	0.5487	0.3314	0.5169	-0.5169
40	Austria	39	44	13	4	0.5680	0.3264	-1.7347	1.7347
41	Swiss	42	47	8	3	0.5049	0.1976	-0.5218	0.5218
42	Italy	45	40	11	4	0.4547	0.2993	0.1149	-0.1149
43	North Italy	42	43	11	4	0.5034	0.2842	-0.4132	0.4132
44	South Italy	46	35	15	4	0.4510	0.4343	-0.6086	0.6086
45	Czech	33	41	18	8	0.6372	0.4546	0.0197	-0.0197
46	Hungary	30	43	19	8	0.7223	0.4626	-1.7437	1.7437
47	*Gypsies	30	25	36	9	0.7213	0.9376	-1.6902	1.6902
48	Poland	35	38	19	8	0.5951	0.4987	0.5608	-0.5608
49	Yugoslavia	37	42	14	7	0.5534	0.3600	1.2048	-1.2048
50	Romania	34	45	17	7	0.7083	0.4097	-4.9869	1.9869
51	Bulgaria	32	44	16	8	0.6502	0.3934	0.2636	-0.2636
52	Albania	42	36	17	5	0.5078	0.4725	-0.7220	0.7220
53	Greece	43	39	13	5	0.4778	0.3547	0.4094	-0.4094
54	Cyprus	35	46	13	6	0.6088	0.3174	-0.2807	0.2807
55	Turkey	33	45	15	7	0.6439	0.3665	-0.3693	0.3693
56	Iran(Westnorth)	36	33	24	7	0.6087	0.6484	-1.2738	1.2738
57	Iran(Eastsouth)	42	26	25	7	0.4820	0.7678	1.1033	-1.1033
58	Iran(Middleeast)	31	25	34	10	0.6623	0.9162	0.5671	-0.5671
59	Iraq	35	31	26	8	0.6115	0.7091	-0.4441	0.4441
60	Kuwait	47	24	24	5	0.4291	0.7854	0.0733	-0.0733
61	Lebanon	36	47	12	5	0.6023	0.2907	-0.8845	0.8845
62	Israel	36	41	17	6	0.6092	0.4332	-1.3042	1.3042

TABLE III. COUNTRY.1-1 This table shows available **experimental data** of blood type ratios for 62 different countries around the world, where totally 114 different countries' data are available [13]. To be continued to TABLE IV.

Index	Country	$O_{exp}(\%)$	$A_{exp}(\%)$	$B_{exp}(\%)$	$AB_{exp}(\%)$	θ_1	θ_2	Diff%($O_t - O_{exp}$)	Diff%($AB_t - AB_{exp}$)
63	Pakistan	31	25	34	10	0.6623	0.9162	0.5671	-0.5671
64	Afgjanistan	29	25	36	10	0.7213	0.9376	-0.6902	0.6902
65	India(Westnorth)	29	21	41	9	0.7349	1.0549	-1.4084	1.4084
66	India(Eastnorth)	32	25	36	7	0.7213	0.9376	-3.6902	3.6902
67	India(Middlesouth)	37	22	34	7	0.5813	0.9719	-0.5815	0.5815
68	Srilanka	47	22	26	5	0.4286	0.8609	0.1098	-0.1098
69	Myanmar	35	25	32	8	0.6103	0.8921	-0.3710	0.3710
70	Thailand	39	22	33	6	0.5594	0.9605	-1.1801	1.1801
71	Malaysia	38	25	29	8	0.5418	0.8508	0.9718	-0.9718
72	Philippines	45	26	24	5	0.4635	0.7494	-0.5460	0.5460
73	Vietnam	42	22	31	5	0.5183	0.9357	-1.4429	1.4429
74	Cambodia	39	23	35	3	0.6313	0.9636	-5.6284	5.6284
75	South China	44	27	23	6	0.4631	0.7135	0.4828	-0.4828
76	North China	33	30	29	8	0.6671	0.7708	-1.7025	1.7025
77	Middle China	35	32	26	7	0.6371	0.6960	-1.9711	1.9711
78	Hong Kong	44	24	26	6	0.4635	0.8214	0.4540	-0.4540
79	Macao	40	25	28	7	0.5210	0.8357	0.3689	-0.3689
80	Tibet	30	37	24	9	0.7180	0.6056	-1.5096	1.5096
81	Taiwan	44	27	23	6	0.4631	0.7135	0.4828	-0.4828
82	Nepal	30	37	24	9	0.7180	0.6056	-1.5096	1.5096
83	Mongolia	37	22	34	7	0.5813	0.9719	-0.5815	0.5815
84	South Korea	27	32	30	11	0.7656	0.7584	-1.0020	1.0020
85	Japan	31	38	22	9	0.6810	0.5591	-0.4866	0.4866
86	Sumatra	41	23	30	6	0.5195	0.9025	-0.5264	0.5264
87	Java	37	26	29	8	0.5642	0.8334	0.5067	-0.5067
88	Middle Asia(Russia)	32	28	31	9	0.6666	0.8291	-0.6754	0.6754
89	Sibereria(Russia)	39	25	29	7	0.5418	0.8508	-0.0282	0.0282
90	Russia(Europe)	34	35	23	8	0.6313	0.6072	-0.6284	0.6284
91	Caucasus	44	32	20	4	0.4961	0.5810	-1.9009	1.9009
92	Georgia	50	36	11	4	0.3960	0.3239	-0.2710	-0.7290
93	Armenia	29	50	13	8	0.7012	0.3027	0.3995	-0.3995
94	Egypt	34	34	24	8	0.6336	0.6367	-0.7674	0.7674
95	Libya	40	36	19	5	0.5522	0.5166	-1.7167	1.7167
96	Tunisia	46	31	18	5	0.4409	0.5485	0.1610	-0.1610
97	Algelia	44	39	13	4	0.4778	0.3547	-0.5906	0.5906
98	Morocco	37	34	23	6	0.6067	0.6181	-2.1529	2.1529
99	Ethiopia	47	28	21	4	0.4445	0.6568	-1.1176	1.1176
100	Somalia	58	26	13	3	0.2982	0.4818	0.5078	-0.5078
101	Chad	45	27	26	2	0.5213	0.7686	-4.6521	4.6521
102	Senegal	50	25	21	4	0.3967	0.7061	-0.3307	0.3307
103	Libelia	46	25	24	5	0.4460	0.7670	-0.2296	0.2296
104	Ghana	49	22	25	4	0.4126	0.8435	-0.6182	0.6182
105	Cameroon	54	22	21	3	0.3533	0.7640	-0.6282	0.6282
106	Congo	49	27	20	4	0.4114	0.6504	-0.5293	0.5293
107	Guinea	64	17	17	2	0.2450	0.7854	0.0000	0.0000
108	Angola	49	25	22	4	0.4126	0.7273	-0.6182	0.6182
109	Uganda	49	23	23	5	0.3971	0.7854	0.6345	-0.6345
110	Mozambique	57	23	17	3	0.3131	0.6465	0.0677	-0.0677
111	Madagascar	43	23	28	6	0.4812	0.8731	0.1624	-0.1624
112	Sorth Africa	45	35	16	4	0.4699	0.4584	-1.0201	1.0201
113	Kenya	49	26	22	3	0.4286	0.7099	-1.8902	1.8902
114	Zambia	45	25	27	3	0.5011	0.8197	-3.2547	3.2547

TABLE IV. COUNTRY.1-2. This table shows available **experimental data** of blood type ratios for another 52 different countries around the world, where totally 114 different countries' data are available [13], continued from TABLE III. Be aware that each country may consist of many different ethnic groups, so these fittings are some approximate examples. For a country with multi-ethnicities such as USA, the theoretical prediction does not work as well as a country with a pure ethnic group.

Index	Country	$O_t(\%)$	$AA_t(\%)$	$Ai_t(\%)$	$BB_t(\%)$	$Bi_t(\%)$	$AB_t(\%)$	Error $\%(\frac{O_t - O_{exp}}{O_{exp}})$	Error $\%(\frac{AB_t - AB_{exp}}{AB_{exp}})$
1	Canada	40.74	8.28	36.72	0.55	9.45	4.26	-0.63	6.50
2	USA	45.39	6.54	34.46	0.50	9.50	3.61	0.87	-9.83
3	Mexico	84.75	0.34	10.66	0.05	3.95	0.25	0.89	-75.12
4	Guatemala	94.97	0.02	2.98	0.01	1.99	0.03	-0.03	
5	El Salvador	60.95	2.30	23.70	0.46	10.54	2.05	1.58	-31.68
6	Nicaragua	91.96	0.13	6.87	0.00	1.00	0.04	-0.04	
7	Costa Rica	52.81	3.56	27.44	0.71	12.29	3.19	-0.36	6.38
8	Cuba	48.36	4.98	31.02	0.66	11.34	3.64	-1.30	21.19
9	Jamaica	55.80	1.53	18.47	1.67	19.33	3.20	-0.35	6.63
10	Dominican Rep	52.81	3.56	27.44	0.71	12.29	3.19	-0.36	6.38
11	Haiti	51.07	2.85	24.15	1.36	16.64	3.93	0.13	-1.63
12	Puerto Rico	53.96	3.30	26.70	0.70	12.30	3.04	14.80	-69.57
13	Colombia	62.28	2.42	24.58	0.30	8.70	1.72	0.46	-14.22
14	Ecuador	63.79	2.71	26.29	0.13	5.87	1.21	1.26	-39.57
15	Peru	70.90	1.13	17.87	0.27	8.73	1.10	-0.14	10.06
16	Chile	56.66	3.37	27.63	0.41	9.59	2.34	1.18	-22.02
17	Bolivia	92.95	0.07	4.93	0.01	1.99	0.05	-0.06	
18	Venezuela	44.38	5.57	31.43	0.96	13.04	4.62	0.87	-7.63
19	Brazil	47.68	5.78	33.22	0.48	9.52	3.32	-0.66	10.58
20	Argentina	47.68	5.78	33.22	0.48	9.52	3.32	-0.66	10.58
21	Paraguay	54.63	4.09	29.91	0.34	8.66	2.37	-2.45	136.96
22	Uruguay	44.24	6.94	35.06	0.51	9.49	3.76	-1.69	25.34
23	Australia	46.54	6.15	33.85	0.49	9.51	3.46	-0.98	15.31
24	New Zealand	47.95	6.02	33.98	0.39	8.61	3.05	-0.11	1.73
25	Iceland	55.55	3.62	28.38	0.41	9.59	2.45	-0.80	22.42
26	Ireland	54.44	3.89	29.11	0.42	9.58	2.56	0.81	-14.64
27	United Kingdom	46.82	6.39	34.61	0.40	8.60	3.18	-0.38	6.00
28	Scotland	50.87	4.56	30.44	0.54	10.46	3.13	-0.26	4.36
29	England	46.00	7.03	35.97	0.32	7.68	3.00	-0.01	0.08
30	Norway	39.18	9.80	39.20	0.37	7.63	3.82	0.47	-4.61
31	Sweden	38.37	9.27	37.73	0.58	9.42	4.63	0.97	-7.36
32	Finland	31.59	8.75	33.25	2.02	15.98	8.41	-4.27	20.14
33	Denmark	41.91	7.81	36.19	0.53	9.47	4.09	-0.21	2.16
34	Netherlands	44.55	7.19	35.81	0.41	8.59	3.45	-1.00	15.02
35	Belgium	46.00	7.03	35.97	0.32	7.68	3.00	-0.01	0.08
36	France	42.26	8.07	36.93	0.43	8.57	3.74	-1.73	24.77
37	Spain	42.26	8.07	36.93	0.43	8.57	3.74	0.61	-6.42
38	Portugal	40.33	9.29	38.71	0.36	7.64	3.67	-1.62	22.18
39	Germany	38.52	7.97	35.03	0.94	12.06	5.48	1.36	-8.62
40	Austria	37.27	8.47	35.53	0.97	12.03	5.73	-4.45	43.37
41	Swiss	41.48	8.80	38.20	0.35	7.65	3.52	-1.24	17.39
42	Italy	45.11	6.30	33.70	0.60	10.40	3.89	0.26	-2.87
43	North Italy	41.59	7.55	35.45	0.64	10.36	4.41	-0.98	10.33
44	South Italy	45.39	4.97	30.03	1.07	13.93	4.61	-1.32	15.22
45	Czech	33.02	8.16	32.84	1.95	16.05	7.98	0.06	-0.25
46	Hungary	28.26	9.77	33.23	2.43	16.57	9.74	-5.81	21.80
47	*Gypsies	28.31	3.92	21.08	7.28	28.72	10.69	-5.63	18.78
48	Poland	35.56	6.83	31.17	2.03	16.97	7.44	1.60	-7.01
49	Yugoslavia	38.20	7.70	34.30	1.09	12.91	5.80	3.26	-17.21
50	Romania	29.01	10.35	34.65	1.95	15.05	8.99	-14.67	28.38
51	Bulgaria	32.26	9.32	34.68	1.61	14.39	7.74	0.82	-3.30
52	Albania	41.28	5.60	30.40	1.46	15.54	5.72	-1.72	14.44
53	Greece	43.41	6.20	32.80	0.85	12.15	4.59	0.95	-8.19
54	Cyprus	34.72	9.56	36.44	1.03	11.97	6.28	-0.80	4.68
55	Turkey	32.63	9.60	35.40	1.41	13.59	7.37	-1.12	5.28
56	Iran(Westnorth)	34.73	5.46	27.54	3.13	20.87	8.27	-3.54	18.20
57	Iran(Eastsouth)	43.10	3.05	22.95	2.85	22.15	5.90	2.63	-15.76
58	Iran(Middleeast)	31.57	3.62	21.38	6.14	27.86	9.43	1.83	-5.67
59	Iraq	34.56	4.92	26.08	3.62	22.38	8.44	-1.27	5.55
60	Kuwait	47.07	2.46	21.54	2.46	21.54	4.93	0.16	-1.47
61	Lebanon	35.12	9.83	37.17	0.88	11.12	5.88	-2.46	17.69
62	Israel	34.70	7.90	33.10	1.69	15.31	7.30	-3.62	21.74

TABLE V. COUNTRY.2-1 This table shows our **theoretical prediction** of blood type ratios for 62 different countries around the world. The theoretical prediction here in TABLE V is compared to the experimental data in TABLE III. To be continued to TABLE VI

Index	Country	$O_t(\%)$	$AA_t(\%)$	$Ai_t(\%)$	$BB_t(\%)$	$Bi_t(\%)$	$AB_t(\%)$	Error%($\frac{O_t - O_{exp}}{O_{exp}}$)	Error%($\frac{AB_t - AB_{exp}}{AB_{exp}}$)
63	Pakistan	31.57	3.62	21.38	6.14	27.86	9.43	1.83	-5.67
64	Afgjanistan	28.31	3.92	21.08	7.28	28.72	10.69	-2.38	6.90
65	India(Westnorth)	27.59	2.95	18.05	9.18	31.82	10.41	-4.86	15.65
66	India(Eastnorth)	28.31	3.92	21.08	7.28	28.72	10.69	-11.53	52.72
67	India(Middlesouth)	36.42	2.59	19.41	5.55	28.45	7.58	-1.57	8.31
68	Srilanka	47.11	2.10	19.90	2.85	23.15	4.89	0.23	-2.20
69	Myanmar	34.63	3.38	21.62	5.19	26.81	8.37	-1.06	4.64
70	Thailand	37.82	2.51	19.49	5.13	27.87	7.18	-3.03	19.67
71	Malaysia	38.97	3.08	21.92	4.01	24.99	7.03	2.56	-12.15
72	Philippines	44.45	2.98	23.02	2.58	21.42	5.55	-1.21	10.92
73	Vietnam	40.56	2.37	19.63	4.37	26.63	6.44	-3.44	28.86
74	Cambodia	33.37	3.00	20.00	6.21	28.79	8.63	-14.43	187.61
75	South China	44.48	3.19	23.81	2.39	20.61	5.52	1.10	-8.05
76	North China	31.30	4.99	25.01	4.71	24.29	9.70	-5.16	21.28
77	Middle China	33.03	5.37	26.63	3.75	22.25	8.97	-5.63	28.16
78	Hong Kong	44.45	2.58	21.42	2.98	23.02	5.55	1.03	-7.57
79	Macao	40.37	3.00	22.00	3.67	24.33	6.63	0.92	-5.27
80	Tibet	28.49	7.59	29.41	3.64	20.36	10.51	-5.03	16.77
81	Taiwan	44.48	3.19	23.81	2.39	20.61	5.52	1.10	-8.05
82	Nepal	28.49	7.59	29.41	3.64	20.36	10.51	-5.03	16.77
83	Mongolia	36.42	2.59	19.41	5.55	28.45	7.58	-1.57	8.31
84	South Korea	26.00	6.33	25.67	5.69	24.31	12.00	-3.71	9.11
85	Japan	30.51	7.58	30.42	2.97	19.03	9.49	-1.57	5.41
86	Sumatra	40.47	2.58	20.42	4.13	25.87	6.53	-1.28	8.77
87	Java	37.51	3.40	22.60	4.12	24.88	7.49	1.37	-6.33
88	Middle Asia(Russia)	31.32	4.43	23.57	5.28	25.72	9.68	-2.11	7.50
89	Sibereria(Russia)	38.97	3.08	21.92	4.01	24.99	7.03	-0.07	0.40
90	Russia(Europe)	33.37	6.21	28.79	3.00	20.00	8.63	-1.85	7.85
91	Caucasus	42.10	4.49	27.51	1.94	18.06	5.90	-4.32	47.52
92	Georgia	49.73	4.87	31.13	0.55	10.45	3.27	-0.54	-18.23
93	Armenia	29.40	12.17	37.83	1.19	11.81	7.60	1.38	-4.99
94	Egypt	33.23	5.93	28.07	3.24	20.76	8.77	-2.26	9.59
95	Libya	38.28	5.91	30.09	1.91	17.09	6.72	-4.29	34.33
96	Tunisia	46.16	3.96	27.04	1.48	16.52	4.84	0.35	-3.22
97	Algelia	43.41	6.20	32.80	0.85	12.15	4.59	-1.34	14.77
98	Morocco	34.85	5.73	28.27	2.90	20.10	8.15	-5.82	35.88
99	Ethiopia	45.88	3.32	24.68	1.97	19.03	5.12	-2.38	27.94
100	Somalia	58.51	2.38	23.62	0.65	12.35	2.49	0.88	-16.93
101	Chad	40.35	3.44	23.56	3.22	22.78	6.65	-10.34	232.60
102	Senegal	49.67	2.54	22.46	1.85	19.15	4.33	-0.66	8.27
103	Libelia	45.77	2.71	22.29	2.52	21.48	5.23	-0.50	4.59
104	Ghana	48.38	2.06	19.94	2.59	22.41	4.62	-1.26	15.46
105	Cameroon	53.37	1.89	20.11	1.74	19.26	3.63	-1.16	20.94
106	Congo	48.47	2.98	24.02	1.72	18.28	4.53	-1.08	13.23
107	Guinea	64.00	1.00	16.00	1.00	16.00	2.00	0.00	0.00
108	Angola	48.38	2.59	22.41	2.06	19.94	4.62	-1.26	15.46
109	Uganda	49.63	2.18	20.82	2.18	20.82	4.37	1.29	-12.69
110	Mozambique	57.07	1.94	21.06	1.11	15.89	2.93	0.12	-2.26
111	Madagascar	43.16	2.45	20.55	3.48	24.52	5.84	0.38	-2.71
112	Sorth Africa	43.98	5.09	29.91	1.24	14.76	5.02	-2.27	25.50
113	Kenya	47.11	2.85	23.15	2.10	19.90	4.89	-3.86	63.01
114	Zambia	41.75	2.92	22.08	3.35	23.65	6.25	-7.23	108.49

TABLE VI. COUNTRY.2-2. This table shows our **theoretical prediction** of blood type ratios for another 52 different countries around the world, continued from TABLE V. The theoretical prediction here in TABLE VI is compared to the experimental data in TABLE IV

IV. GENERAL GENE-MATING EVOLUTION MODEL AND THEORY

A. Governing equations, stable equilibrium solutions and exact analytic solutions

We can generalize our model and theory of Sec. III to $n+1$ alleles. Alternatively, one may say n dominant alleles and 1 recessive allele in a single locus. For dominant gene with a label α , we denote it as D_α ; and for the only recessive gene we denote as r . We denote biological traits of $D_\alpha D_\alpha$ as $G_{\alpha\alpha}$, $D_\alpha D_\beta$ as $G_{\alpha\beta}$ ($\equiv G_{\beta\alpha}$) for $\alpha \neq \beta$, $D_\alpha r$ as $G_{\alpha 0}$ ($\equiv G_{0\alpha}$), rr as G_{00} ($\equiv G_{00}$). Indeed, whether the genotypes we studied have dominant or recessive alleles do not matter, we can simply label them as $G_{\alpha\beta}$ generically. We derive the governing equations for *population parameters* as:

$$\begin{cases} \frac{d}{dt} G_{\alpha\alpha} = k_b \frac{1}{P} (G_{\alpha\alpha} \sum_{j=0}^n G_{\alpha j} + \frac{1}{4} \sum_{i=0}^n \sum_{j=0}^n G_{\alpha i} G_{\alpha j} - k_d G_{\alpha\alpha}), \\ \frac{d}{dt} G_{\alpha\beta} = k_b \frac{1}{P} (2G_{\alpha\alpha} G_{\beta\beta} + \sum_{i=0}^n G_{\alpha i} G_{\beta\beta} \\ + \sum_{j=0}^n G_{\alpha\alpha} G_{\beta j} + \frac{1}{2} \sum_{i=0}^n \sum_{j=0}^n G_{\alpha i} G_{\beta j}) - k_d G_{\alpha\beta}. \end{cases} \quad (22)$$

By redefining a *population parameters* G to the *percentages parameter* $\frac{G}{P} \rightarrow G$, we derive the governing equations for *percentages parameters* as:

$$\begin{cases} \frac{d}{dt} G_{\alpha\alpha} = k_b (G_{\alpha\alpha} \sum_{j=0}^n G_{\alpha j} + \frac{1}{4} \sum_{i=0}^n \sum_{j=0}^n G_{\alpha i} G_{\alpha j} - G_{\alpha\alpha}), \\ \frac{d}{dt} G_{\alpha\beta} = k_b (2G_{\alpha\alpha} G_{\beta\beta} + \sum_{i=0}^n G_{\alpha i} G_{\beta\beta} \\ + \sum_{j=0}^n G_{\alpha\alpha} G_{\beta j} + \frac{1}{2} \sum_{i=0}^n \sum_{j=0}^n G_{\alpha i} G_{\beta j} - G_{\alpha\beta}). \end{cases} \quad (23)$$

The equilibrium solutions consist of a continuous n -dimensional manifold as a continuous set of fixed-points:

$$\begin{cases} G_{\alpha\alpha,eq}(\theta_k) = [\prod_{i=1}^{\alpha} \frac{\sin^2(\theta_i)}{(\cos(\theta_i) + \sin(\theta_i))^2}] \frac{\cos^2(\theta_{\alpha+1})}{(\cos(\theta_{\alpha+1}) + \sin(\theta_{\alpha+1}))^2}, \\ G_{\alpha\beta,eq}(\theta_k) = [\prod_{i=1}^{\alpha} \frac{\sin^2(\theta_i)}{(\cos(\theta_i) + \sin(\theta_i))^2}] \frac{2 \sin(\theta_{\alpha+1}) \cos(\theta_{\alpha+1})}{(\cos(\theta_{\alpha+1}) + \sin(\theta_{\alpha+1}))^2} \\ \cdot [\prod_{j=1}^{\beta-\alpha-1} \frac{\sin(\theta_{\alpha+1+j})}{\cos(\theta_{\alpha+1+j}) + \sin(\theta_{\alpha+1+j})}] \frac{\cos(\theta_{\beta+1})}{\cos(\theta_{\beta+1}) + \sin(\theta_{\beta+1})}. \end{cases} \quad (24)$$

We are confident to anticipate that the linear stability analysis of the system would give n eigenvalues 0, and $\binom{n+1}{2}$ eigenvalues -1 [14]. Note that $\hat{G}_{\alpha\alpha} + \hat{G}_{\beta\beta} - 2\hat{G}_{\alpha\beta} \equiv \hat{s}_{\alpha\beta}$ (while symmetrically we define $s_{ij} \equiv s_{ji}$) would be the eigenvectors corresponding to -1 eigenvalues. We can parameterize the whole space of G_{ij} ($n+1 + \binom{n+1}{2}$ -dimensions with one constraint) by a new set of $n + \binom{n+1}{2}$

coordinates θ_k, s_{ij} :

$$\begin{cases} G_{\alpha\alpha} = G_{\alpha\alpha,eq}(\theta_k) + \sum_{i=0, i \neq \alpha}^n s_{\alpha i}, \\ G_{\alpha\beta} = G_{\alpha\beta,eq}(\theta_k) - 2s_{\alpha\beta}. \end{cases} \quad (25)$$

The inverse transformation is:

$$\begin{cases} \theta_k = \tan^{-1} \{ [\sum_{i=k}^n (2G_{ii} + \sum_{j=0, j \neq i}^n G_{ij})] / (2G_{k-1,k-1} + \sum_{j=0, j \neq k-1}^n 2G_{k-1,j}) \}, \\ 1 \leq k \leq n, \text{ totally } n \text{ equations.} \\ s_{ij} \text{ can be solved from the following equations:} \\ \tan^2(\theta_k) = \frac{\sum_{k \leq i \leq j \leq n} G_{ij} - \sum_{i=k}^n \sum_{j=0}^{k-1} s_{ij}}{(G_{k-1,k-1} - \sum_{i=0, i \neq k-1}^n s_{k-1,i})}, \\ 1 \leq k \leq n, \text{ totally } n \text{ equations.} \\ \tan(\theta_k) = [\sum_{i=k}^n (G_{mi} + 2s_{mi})] / (G_{m,k-1} + 2s_{m,k-1}), \\ 1 \leq k \leq n, 0 \leq m \leq k-2, \text{ totally } \binom{n}{2} \text{ equations.} \end{cases} \quad (26)$$

Substitute Eq.(25) into Eq.(23), we have the decoupled governing linear equations in the new coordinates:

$$\begin{cases} \frac{ds_{ij}}{dt} = -k_b s_{ij}, \quad 0 \leq i, j \leq n. \\ \frac{d\theta_k}{dt} = 0, \quad 1 \leq k \leq n. \end{cases} \quad (27)$$

Given initial values \tilde{G}_{ij} in the percentage parameter space, the exact analytic solution under time evolution is

$$\begin{aligned} \sum_{0 \leq i \leq j \leq n} G_{ij}(t) \hat{G}_{ij} &= \sum_{0 \leq i \leq j \leq n} G_{ij,eq}(\theta_i = \tilde{\theta}_i) \hat{G}_{ij} \\ &+ \sum_{0 \leq \alpha < \beta \leq n} \tilde{s}_{\alpha\beta} e^{-k_b t} (\hat{G}_{\alpha\alpha} + \hat{G}_{\beta\beta} - 2\hat{G}_{\alpha\beta}). \end{aligned} \quad (28)$$

where $\tilde{\theta}_i$ and $\tilde{s}_{\alpha\beta}$ can be solved in the form of \tilde{G}_{ij} from Eq.(26). **The key to obtain our exact analytic solution is to transform the nonlinear coupled Eq.(23) to the decoupled linear Eq.(27).**

The dimensionality: We explain again the physical meaning on the dimensionality of the fibers and the stable base manifold, shown in Fig.1. For Eq.(23), there is a permutation symmetric group S_{n+1} symmetry by permuting $G_{\alpha\beta}$. The S_{n+1} symmetry also results in time-independent $n+1$ conserved quantities, spanned

by $(2G_{k-1,k-1} + \sum_{j=0, j \neq k-1}^n 2G_{k-1,j})$ with $k = 1, \dots, n+1$.

Since there is a 1-dimensional constraint $\sum G_{jk} = 1$, overall there is n independent degrees of freedom. We can say the S_{n+1} symmetry results in the dimensionality of fixed-point solutions is n , here parametrized by $\theta_1, \dots, \theta_n$. The stable equilibrium base manifold is n -dimensional, the fibers are $\binom{n+1}{2}$ -dimensional.

The geodesic distance as the genetic distance: Again, as stated in Sec.III B 3, we can solve the geodesic distance of two populations on the manifold Eq.(24) in the genotype frequency space to define the genetic distance of two populations. Note that the intrinsic metric $g_{\theta_\mu, \theta_\nu}$ can be derived from

$$\begin{aligned} ds^2 &= \sum_{0 \leq i \leq n; i \leq j \leq n} (dG_{ij}(\theta_1, \dots, \theta_n))^2 \\ &\equiv \sum_{\mu, \nu=1, \dots, n} g_{\theta_\mu, \theta_\nu} d\theta_\mu d\theta_\nu. \end{aligned} \quad (29)$$

The geodesic is solved from the geodesic equation on the manifold Eq.(24):

$$\frac{d^2 \theta_\mu}{ds^2} + \Gamma_{\nu\lambda}^\mu \frac{d\theta_\nu}{ds} \frac{d\theta_\lambda}{ds} = 0 \quad (30)$$

with $\Gamma_{\nu\lambda}^\mu \equiv \frac{1}{2} g^{\mu\rho} (\partial_\nu g_{\lambda\rho} + \partial_\lambda g_{\nu\rho} - \partial_\rho g_{\nu\lambda})$ is the Christoffel symbol.

B. 1-1 mapping and the well-defined manifold

Recall that in Sec.III B, we are aware that in order to have an one-to-one (denoted as 1-1) mapping, we have to specify the valid domain of (θ_1, θ_2) . From Eq.(11), $(\theta_1 = 0, \forall \theta_2)$ would map to $o = 1$ case, this is many-to-one mapping. Topologically we could shrink $(\theta_1 = 0, \forall \theta_2)$ as a point to make it a well-defined 1-1 mapping 2-dimensional manifold. Similarly, we should perform an analogous operation on the general case of Eq.(24):

$$\left\{ \begin{array}{l} \theta_1 = 0, \forall (\theta_2, \theta_3, \dots, \theta_n) \text{ shrink into a point.} \\ \theta_1 \neq 0, \theta_2 = 0, \forall (\theta_3, \dots, \theta_n) \text{ shrink into a point.} \\ \theta_1 \neq 0, \theta_2 \neq 0, \theta_3 = 0, \forall (\theta_4, \dots, \theta_n) \text{ shrink into a point.} \\ \vdots \\ \theta_1 \neq 0, \theta_2 \neq 0, \dots, \theta_{n-2} \neq 0, \theta_{n-1} = 0, \forall \theta_n \text{ shrink into a point.} \end{array} \right. \quad (31)$$

For the same reason, the inverse functions Eq.(13) and Eq.(26) are not one-to-one defined at those few points. Nonetheless, we could follow the rule of Eq.(31) to make them one-to-one well-defined.

C. Equilibrium solutions as a global attractor, monotonic behavior, non-extinction and the Hardy-Weinberg Law

Now we can prove several fundamental common properties of macroscopic gene-mating dynamical evolutionary systems. Our proofs are straightforward since we have the time-evolutionary analytic solution in Eq.(28).

(1) **The global stability** of the system: as the time approaches infinity (approximately), the LHS parameters of Eq.(28) will evolve to an equilibrium solution through a 1-dimensional line direction $\sum_{0 \leq \alpha < \beta \leq n} s_{\alpha\beta} \hat{s}_{\alpha\beta}$.

(2) **Monotonic:** Time-evolution of parameters in Eq.(28) is also monotonic through the exponential decay along the $\hat{s}_{\alpha\beta}$ direction to the corresponding equilibrium fixed-point on the stable manifold Eq.(24).

(3) **Non-extinction and the Hardy-Weinberg law:** Based on our model, here we further claim that our following non-extinction statement shows a proof of the Hardy-Weinberg law [11, 12] for a gene-mating system.

Our non-extinction statement states that *any genotype or an allele that ever appears in the population will never become extinct*. The Hardy-Weinberg law states that in the absence of other evolutionary influences, the population genetics will obtain an equilibrium.

We prove that our model not only have the stable fixed points as a continuous manifold in Eq.(24), but also verify a stronger claim from a dynamical viewpoint — if there ever exists a certain genotype, no matter how tiny a portion it is in the total population, it will never become extinct under time-evolution. Here is our proof. The extinction evolution approaches zeros for certain genotypes. Zeros are a final state, which must be located at some equilibrium point. This is easy to verify by moving an equilibrium point (those points with a certain genotype percentage equal to zero) away from the equilibrium manifold through the time-reversal evolution direction (the line direction of Eq.(25)). We find that it is impossible because there must be another genotype going to a value less than 0, but the population percentage cannot be smaller than 0 at any moment. The contradiction shows time-evolution never brings genotype frequencies to approach extinction points. We have proven the non-extinction statement and the Hardy-Weinberg law for the genotype frequency.

We can prove the non-extinction for the allele frequency from the fact that *the time-evolution direction in the genotype frequency space always conserves the allele frequency*. Namely, in Eq.(25), along the $(\hat{G}_{\alpha\alpha} + \hat{G}_{\beta\beta} - 2\hat{G}_{\alpha\beta}) \equiv \hat{s}_{\alpha\beta}$ direction on the fiber, the allele frequency is conserved independently of time. We have thus proven the non-extinction statement for both genotype frequencies and allele frequencies.

Based on these three proven facts above, we know the global properties of *genotype frequency* space of the evolutionary system; and we also know the topological properties of *genotype frequency* space from the fiber bundle picture, shown in Fig.1.

V. MUTATION AND NATURAL SELECTION

Let us consider a more generic model beyond Eq.(22) and Eq.(23) to include the process of mutation and natural selection.

Mutation, for example, corresponds to enlarging the parameter space through adding a new gene type (genotypes or alleles). Natural selection, for example, corre-

ponds to perturb the birth rate, the death rate, and the inherited factor of our governing equations. The population governing equations with various independent birth rates k_{bij} and various death rates k_{dij} can be:

$$\left\{ \begin{array}{l} \frac{d}{dt} G_{\alpha\alpha} = \frac{1}{P} (\sqrt{k_{b\alpha\alpha}} G_{\alpha\alpha} \sum_{j=0}^n \sqrt{k_{b\alpha j}} G_{\alpha j} + \\ \quad \frac{1}{4} \sum_{i=0}^n \sum_{\substack{j=0 \\ i \neq \alpha j \neq \alpha}}^n \sqrt{k_{b\alpha i}} G_{\alpha i} \sqrt{k_{b\alpha j}} G_{\alpha j} - k_{d\alpha\alpha} G_{\alpha\alpha}, \\ \frac{d}{dt} G_{\alpha\beta} = \frac{1}{P} (2\sqrt{k_{b\alpha\alpha}} G_{\alpha\alpha} \sqrt{k_{b\beta\beta}} G_{\beta\beta} + \\ \quad \sum_{i=0}^n \sqrt{k_{b\alpha i}} G_{\alpha i} \sqrt{k_{b\beta\beta}} G_{\beta\beta} + \sum_{\substack{j=0 \\ j \neq \beta}}^n \sqrt{k_{b\alpha\alpha}} G_{\alpha\alpha} \sqrt{k_{b\beta j}} G_{\beta j} + \\ \quad \frac{1}{2} \sum_{i=0}^n \sum_{\substack{j=0 \\ i \neq \alpha j \neq \beta}}^n \sqrt{k_{b\alpha i}} G_{\alpha i} \sqrt{k_{b\beta j}} G_{\beta j}) - k_{d\alpha\beta} G_{\alpha\beta}. \end{array} \right. \quad (32)$$

Here we apply the square root of birth rate or death rate, $\sqrt{k_{b\alpha\beta}}$, $\sqrt{k_{d\alpha\beta}}$, to distribute the birth and the death contributions from two genders carrying two independent sets of genes. On one hand, for a consistency check, this could reduce to the original standard equations if both birth and death rates are universal ($\sqrt{k_{b\alpha\beta}} = \sqrt{k_b}$, $\sqrt{k_{d\alpha\beta}} = \sqrt{k_d}$) regardless different of genetic traits. On the other hand, the separated square roots from two genders show the natural selection effect, i.e., the preferred gene or genotype has a strong tendency to bear more offspring. The amount of offspring depends on the population of both genders, and also on the multiplication product of their square root birth rates.

Next we rewrite Eq.(32) in terms of variables $\frac{G}{P}$, where G is any of the population parameters, and then redefine $\frac{G}{P} \rightarrow G$. The governing equations for percentage parameters as *genotype frequencies* for the redefined percentage G are:

$$\left\{ \begin{array}{l} \frac{d}{dt} G_{\alpha\alpha} = (\sqrt{k_{b\alpha\alpha}} G_{\alpha\alpha} \sum_{j=0}^n \sqrt{k_{b\alpha j}} G_{\alpha j} + \\ \quad \frac{1}{4} \sum_{i=0}^n \sum_{\substack{j=0 \\ i \neq \alpha j \neq \alpha}}^n \sqrt{k_{b\alpha i}} G_{\alpha i} \sqrt{k_{b\alpha j}} G_{\alpha j} - k_{d\alpha\alpha} G_{\alpha\alpha}) - \\ \quad G_{\alpha\alpha} (\sum_{0 \leq i \leq j}^n \sqrt{k_{bij}} G_{ij})^2 + G_{\alpha\alpha} (\sum_{0 \leq i \leq j}^n k_{dij} G_{ij}), \\ \frac{d}{dt} G_{\alpha\beta} = (2\sqrt{k_{b\alpha\alpha}} G_{\alpha\alpha} \sqrt{k_{b\beta\beta}} G_{\beta\beta} + \\ \quad \sum_{i=0}^n \sqrt{k_{b\alpha i}} G_{\alpha i} \sqrt{k_{b\beta\beta}} G_{\beta\beta} + \sum_{\substack{j=0 \\ j \neq \beta}}^n \sqrt{k_{b\alpha\alpha}} G_{\alpha\alpha} \sqrt{k_{b\beta j}} G_{\beta j} + \\ \quad \frac{1}{2} \sum_{i=0}^n \sum_{\substack{j=0 \\ i \neq \alpha j \neq \beta}}^n \sqrt{k_{b\alpha i}} G_{\alpha i} \sqrt{k_{b\beta j}} G_{\beta j} - k_{d\alpha\beta} G_{\alpha\beta}) - \\ \quad - G_{\alpha\beta} (\sum_{0 \leq i \leq j}^n \sqrt{k_{bij}} G_{ij})^2 + G_{\alpha\beta} (\sum_{0 \leq i \leq j}^n k_{dij} G_{ij}). \end{array} \right. \quad (33)$$

Neither Eq.(32) nor Eq.(33) are exactly solvable. Further analysis on the phase diagram of the time-evolving parameter space shows that the patterns of time-evolutions and fixed-points vary through tuning

birth rates or death rates. The original continuous manifold of stable equilibrium solutions Eq.(24) will reduce to discrete points once we tune any birth or death rate. This shows that the *symmetry breaking* of governing equations results in the discrete degeneracy of stable solutions.

The discrete degenerated stable solution will become the *sink*, *source*, or *saddle point* of the phase diagram (rather than just an *attractor of stable fixed-points*, as in the previous case in Sec.IV). These bring up more interesting and complicated phenomena, especially for the case with more genes with a larger parameter space.

VI. CONCLUSION

We have proposed a set of time-dependent coupled nonlinear differential equations as the governing equations to describe a class of gene-mating dynamical evolutionary systems within the disciplines of population genetics and evolutionary biology. Our model consists of the set of governing equations derived from the fundamental assumptions in Sec.II. The specific models for 2 alleles and 3 alleles (blood type) evolutionary systems are derived in Sec.III, and the more generic systems with arbitrary $(n+1)$ -alleles with $((n+1) + \binom{n+1}{2})$ -genotypes are studied in Sec.IV. We find the exact analytic solutions for our models, where the solutions show their most generic forms in Sec.IV.

Based on the exact analytic solutions, we have proved the common properties of gene-mating evolutionary systems: (1) global stability, (2) monotonic evolution, and (3) non-extinction and the Hardy-Weinberg law, under the assumption of no mutation and no natural selection.

More generally, our model in Sec.IV describes the phenomena of the many-body reaction or the many-body collision process. In our work, we interpret the governing equations (23) as the population evolution within a given gene pool. It may be possible that one can also extend Eq.(23) as certain chemical compounds reactions in the chemical reaction pools — such as reactions involving enzymes. Another possible interpretation is to regard Eq.(23) as a discretized variant of the Boltzmann equations. Further extensions of our work will be reported elsewhere.

After the completion of our work, by searching for similar studies in the literature, we became aware of a closely relevant model studied in a pioneer work Ref.[10] where they obtain the exact solutions in a different parameterization. There is also a theoretical proof in [15] of a generalized model of Ref.[10], where the birth rates (fertilities) and the death rates of different genotypes need not to be the same.

There is another study in Ref.[16] concerning the

blood groups (blood type) and their Hardy-Weinberg law, nonetheless their perspective is rather different from ours. Ref.[16]’s model is parameterized by phenotype (instead of our genotype) and its model is discrete model (instead of our continuous model).

The new ingredients for our study are the emphasis on stable fixed-point manifold. We believe that our findings of (1) a unified parameterization of the stable manifold together with the time-dependent evolution and (2) the Euclidean fiber bundle description of exact analytic solutions are new to the literature. We hope that our work can contribute to the population genetics and mathematical biology study.

This is the first paper for a sequence of three related studies. The second [17] and the third paper [18] will be reported elsewhere.

VII. ACKNOWLEDGEMENTS

JW would like to thank Mehran Kardar and Leonid Mirny for showing great interests and encouragements, and giving comments. We thank Jeremy England, Hsien-Ching Kao and Matthew Pinson for comments on the manuscript. JW wishes to thank Yih-Yuh Chen and Ning-Ning Pang for comments in 2006, and thank Sze-Bi Hsu for introducing the reference [4] in 2007 and mentioning the alternative approach: Hirsch’s monotone flow, for proving the global stability (our independent proof is in Sec.IV (1)). JW thanks Mehran Kardar, Patrick Lee and Xiao-Gang Wen for encouraging posting the paper.

JW is supported by NSF Grant No. DMR-1005541, NSFC 11074140, NSFC 11274192, the BMO Financial Group and the John Templeton Foundation. Research at Perimeter Institute is supported by the Government of Canada through Industry Canada and by the Province of Ontario through the Ministry of Research. JWC is supported in part by the MOST, NTU-CTS, and the NTU-CASTS of R.O.C.

-
- [1] S. Wright, “Systems of mating,” *Genetics*, **6**, 111-178 (1921); “*Evolution in Mendelian Populations*” *Genetics*, **16**(2): 97159, (1931); and reference therein.
 - [2] R. A. Fisher, “*The Genetical Theory of Natural Selection*,” Clarendon Press, Oxford (1930).
 - [3] J. F. Crow and M. Kimura, “*An Introduction to Population Genetics Theory*,” Harper and Row, New York (1970)
 - [4] Paul Waltman, “*Competition Models in Population Biology*,” Society for Industrial and Applied Mathematics (1983).
 - [5] A. W. F. Edwards, “*Foundations of Mathematical Genetics*,” 2e, Cambridge University Press (2000).
 - [6] W. J. Ewens, “*Mathematical Population Genetics*,” 2e, Springer (2004).
 - [7] G. Mendel, “Versuche über Pflanzenhybriden (Experiments in Plant Hybridization),” *Verhandlungen des naturforschenden Vereines in Brünn*, Bd. IV für das Jahr 1865, Abhandlungen, 347.
 - [8] This model presented here is originated from an independent thought of the first author during his undergrad freshman year. The governing equations and model are derived in 2003. Substantial work is completed and exact solutions are found in 2006. The manuscript presented here is a late update of our 2006’s work aiming to contribute to the academic literature.
 - [9] Charles Robert Darwin, “*On the Origin of Species*,” (1859).
 - [10] T. Nagylaki and J. F. Crow, “*Continuous selective models*,” *Theoretical Population Biology* **5** 257 (1974).
 - [11] G. H. Hardy, “*Mendelian proportions in a mixed population*,” *Science* **28**:4950 (1908).
 - [12] W. Weinberg, “*Über den Nachweis der Vererbung beim Menschen*,” *Jahreshefte des Verein für vaterländische Naturkunde in Württemberg* **64**:368382 (1908).
 - [13] <http://www.human-abo.org/databank/worldmap.html>
<http://www.bloodbook.com/world-abo.html>
 - [14] For physicists who are familiar with the renormalization group procedure, the linear stability analysis here is simply finding the relevancy of small perturbations. For any eigenvalue equal to 0, the perturbation is marginal. For any eigenvalue smaller than 0, the perturbation is irrelevant, namely stable against perturbations. For any eigenvalue larger than 0, the perturbation is relevant, namely unstable against perturbations.
 - [15] Ethan Akin, Joseph M. Szucs, Approaches to the Hardy-Weinberg manifold, *Journal of Mathematical Biology*, Volume 32, Issue 7, pp 633-643 (1994).
 - [16] M.-H. Chung, S. P. Lee, C. K. Kim, and K. Nahm, *Phys. Rev. E* **56**, 865 (1997)
 - [17] Juven Wang, “*Gene-Mating Dynamic Evolution Theory II: exactly solvable N-gender mating generalization*.”
 - [18] Juven Wang, *et al.*, “*Gene-Mating Dynamic Evolution Theory III: exactly solvable many-body Boltzmann equation generalization*.”

VIII. FIGURES

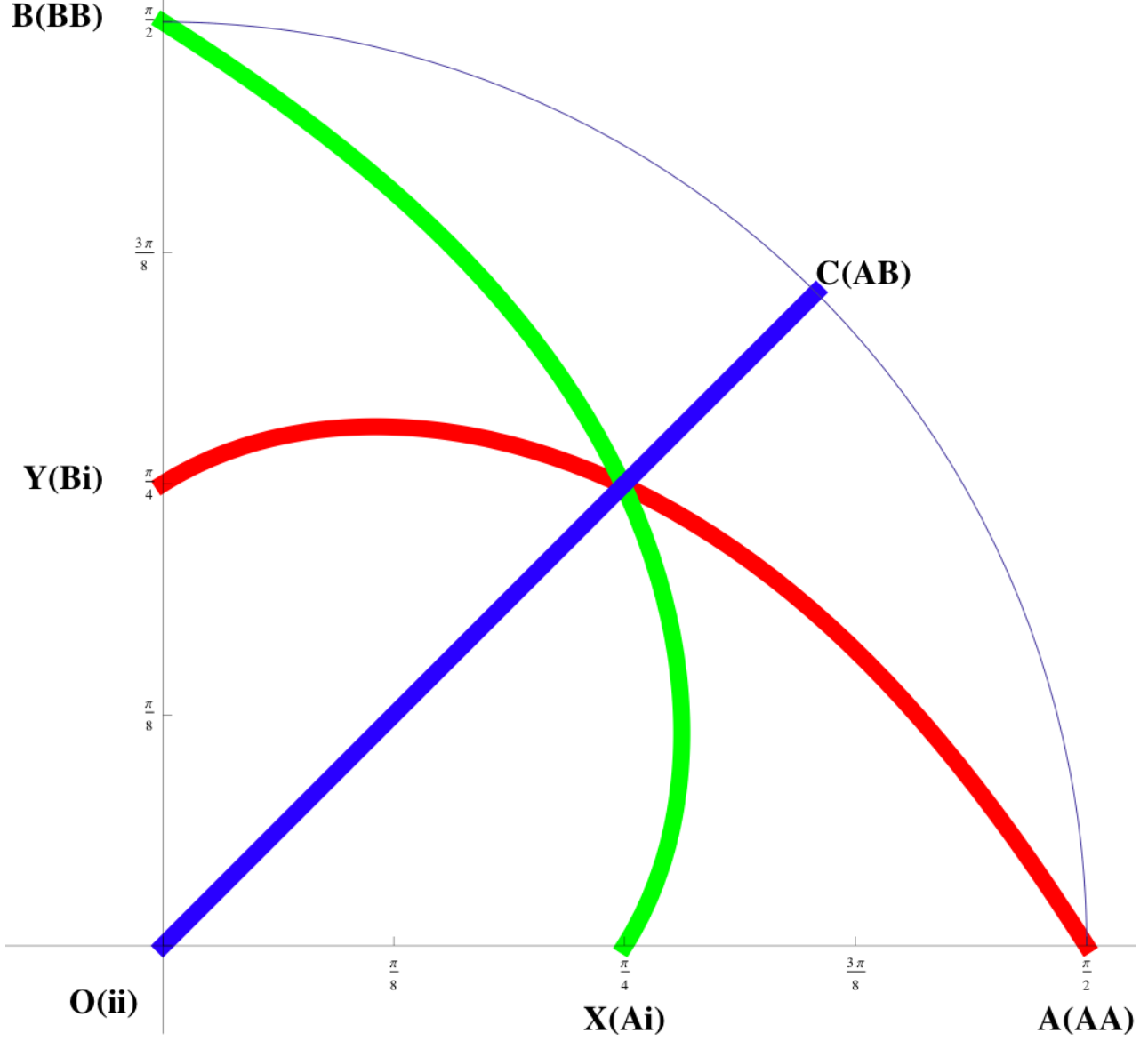
FIG.5. Quadrant $(\theta_1 \cos(\theta_2), \theta_1 \sin(\theta_2))$ for the Blood Type Population Ratio Distribution.

FIG. 5. The quadrant presented here is a 2-dimensional (θ_1, θ_2) parameterization of the 2-dimensional stable equilibrium manifold in Eq.(11) following the description in Sec.III B 2. θ_1 represents the radial direction ($0 \leq \theta_1 \leq \frac{\pi}{2}$), θ_2 represents the angle direction ($0 \leq \theta_2 \leq \frac{\pi}{2}$) of the quadrant. The blue line is $\theta_2 = \frac{\pi}{4}$, reflecting the symmetry invariant under switching x, a to y, b . The green curve is parametrized by $\theta_1(\theta_2) = \frac{(\sqrt{3+\cos(2\theta_2)+2\sin(2\theta_2)}(1+\tan(\theta_2)))}{\sqrt{2+2\sin(2\theta_2)}}$, reflecting the symmetry invariant under switching a, c to o, y . The red curve is parametrized by $\theta_1(\theta_2) = \frac{(\sqrt{3-\cos(2\theta_2)+2\sin(2\theta_2)}(1+\cot(\theta_2)))}{\sqrt{2+2\sin(2\theta_2)}}$, reflecting the symmetry invariant under switching b, c to o, x . The intersection of three color lines, is $(\frac{2}{9}, \frac{2}{9}, \frac{2}{9}, \frac{1}{9}, \frac{1}{9}, \frac{1}{9})$, which is the most symmetric mid point.

FIG.6. Quadrant with the Blood Type Population Ratio Distribution of **World Ethnic Groups** from Table II.

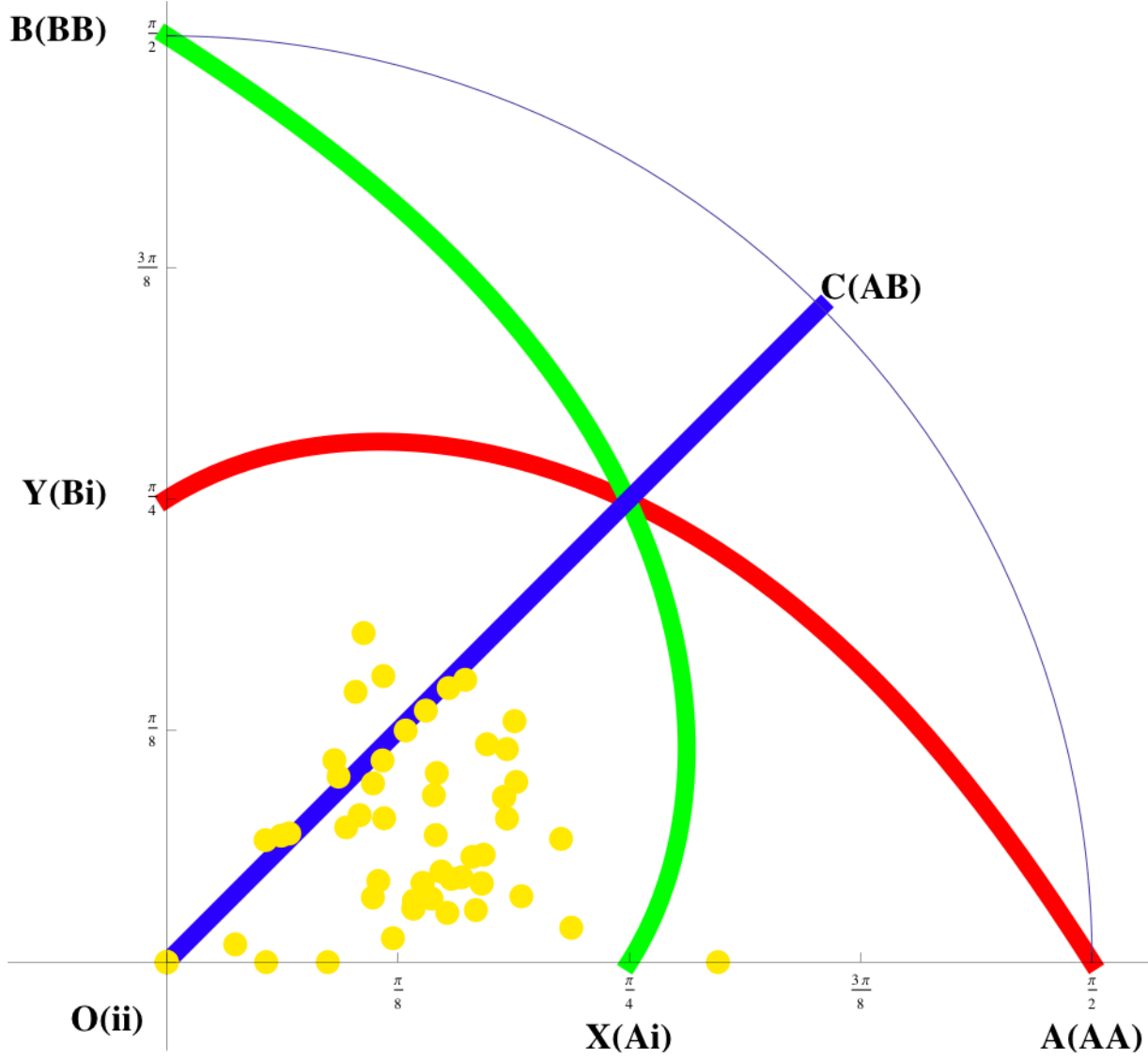


FIG. 6. The quadrant presented here is a 2-dimensional (θ_1, θ_2) parameterization as in FIG.5. We implement our theoretical prediction of the blood type ratio data of ethnic groups in the world from Table II. We plot the theoretical prediction (θ_1, θ_2) distribution of the world ethnic groups from Table II as yellow dots.

FIG.7. Quadrant with the Blood Type Population Ratio Distribution of **World Ethnic Groups** from Table II.

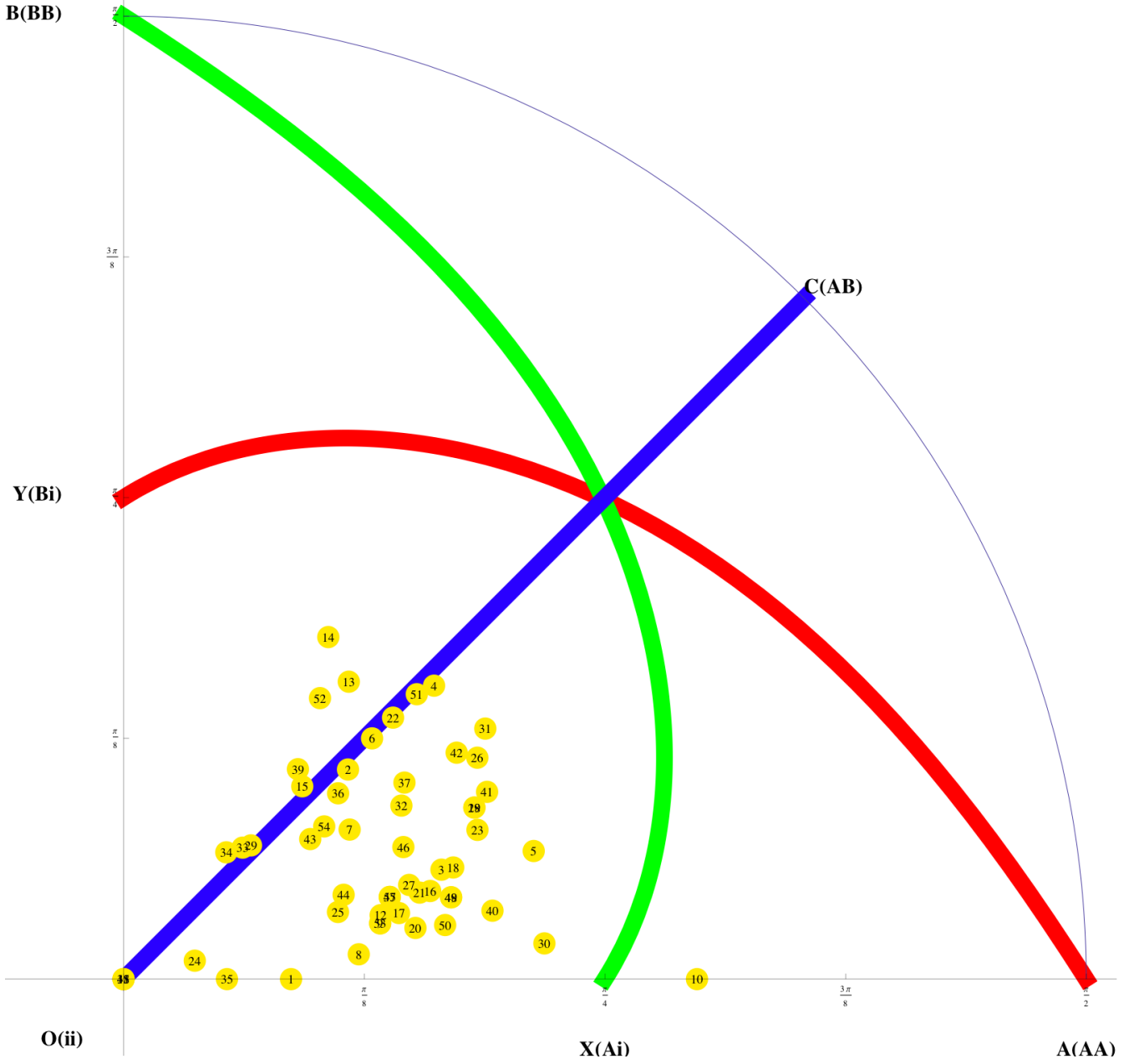


FIG. 7. Similar to FIG.6. The quadrant presented here is a 2-dimensional (θ_1, θ_2) parameterization as in FIG.5. We implement our theoretical prediction of the blood type ratio data of ethnic groups in the world from Table II. We plot the theoretical prediction (θ_1, θ_2) distribution of the world ethnic groups from Table II as yellow dots. The numbers in the yellow dots specify the ethnic groups, numbered in the far-left column of Table II.

FIG.8. Quadrant with the Blood Type Population Ratio Distribution of **World Ethnic Groups** from Table II.

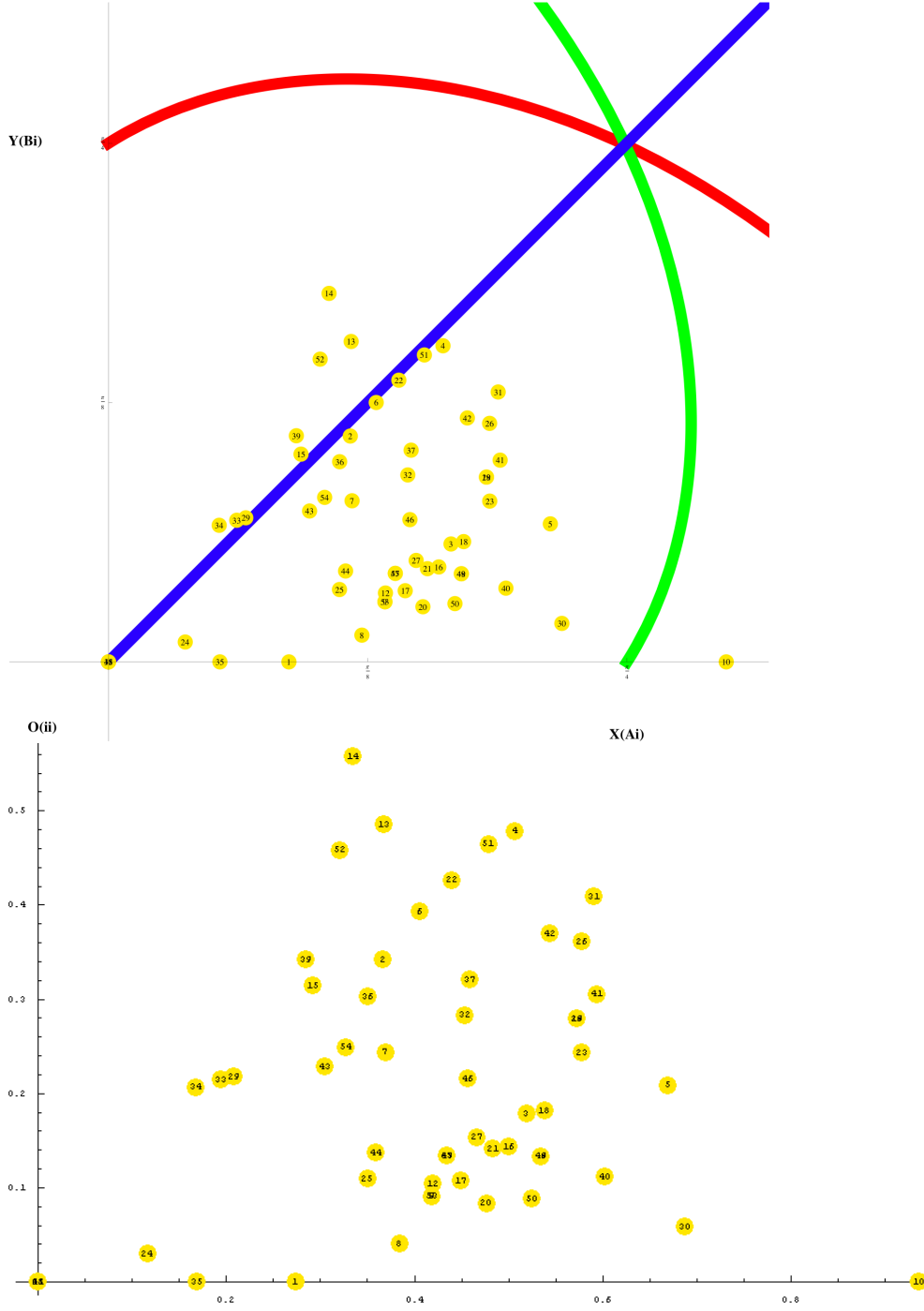


FIG. 8. The zoom-in view of FIG.7. The set up is the same as FIG.7. We implement our theoretical prediction of the blood type ratio data of ethnic groups in the world from Table II.

FIG. 9. Quadrant with the Blood Type Population Ratio Distribution by **Countries** from Table V, VI.

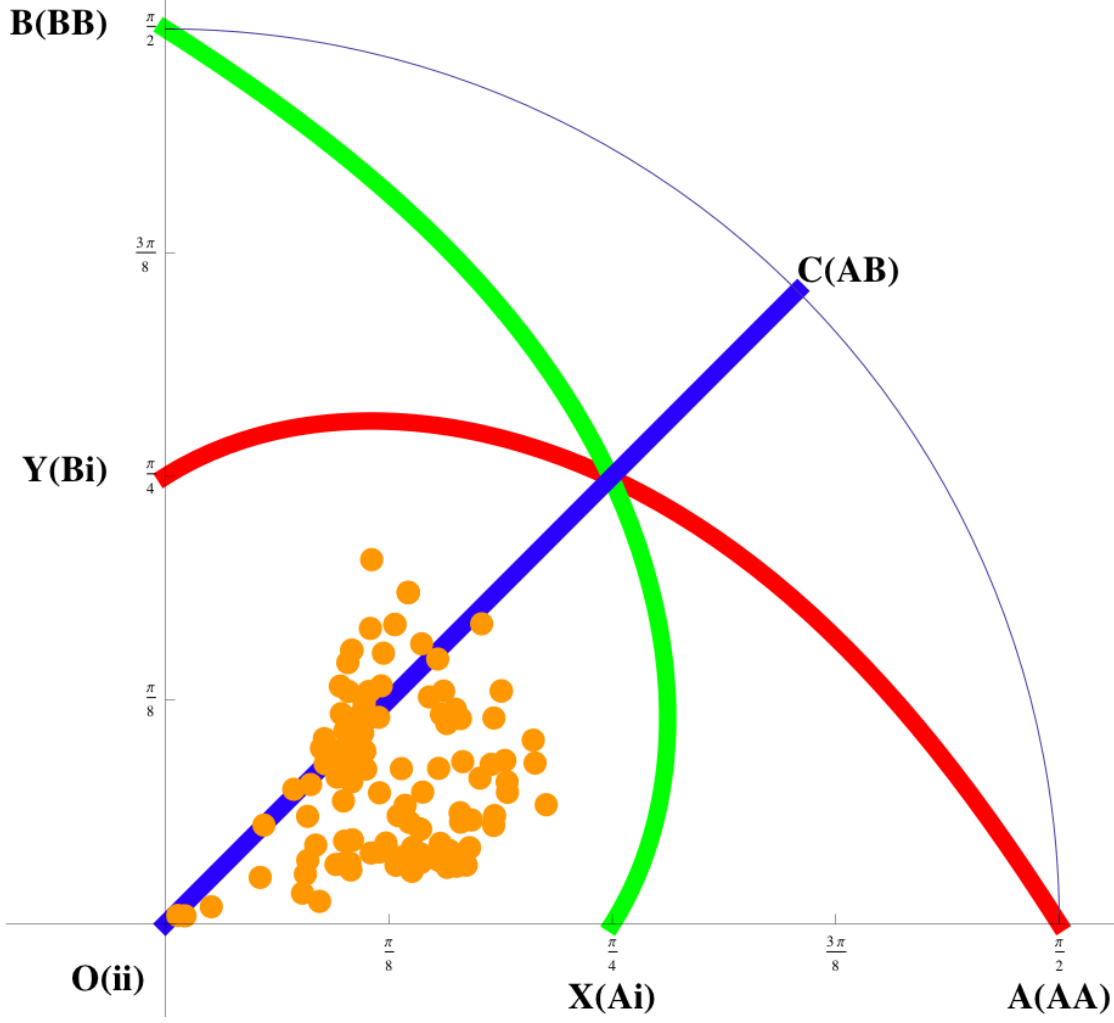


FIG. 9. The quadrant presented here is a 2-dimensional (θ_1, θ_2) parameterization as in FIG. 5. We implement our theoretical prediction of the blood type ratio data of 114 countries in the world from Table V, VI. We plot the theoretical prediction (θ_1, θ_2) distribution of the world ethnic groups from Table V, VI as orange dots.

FIG.10. Quadrant with the Blood Type Population Ratio Distribution by **Countries** from Table V,VI.

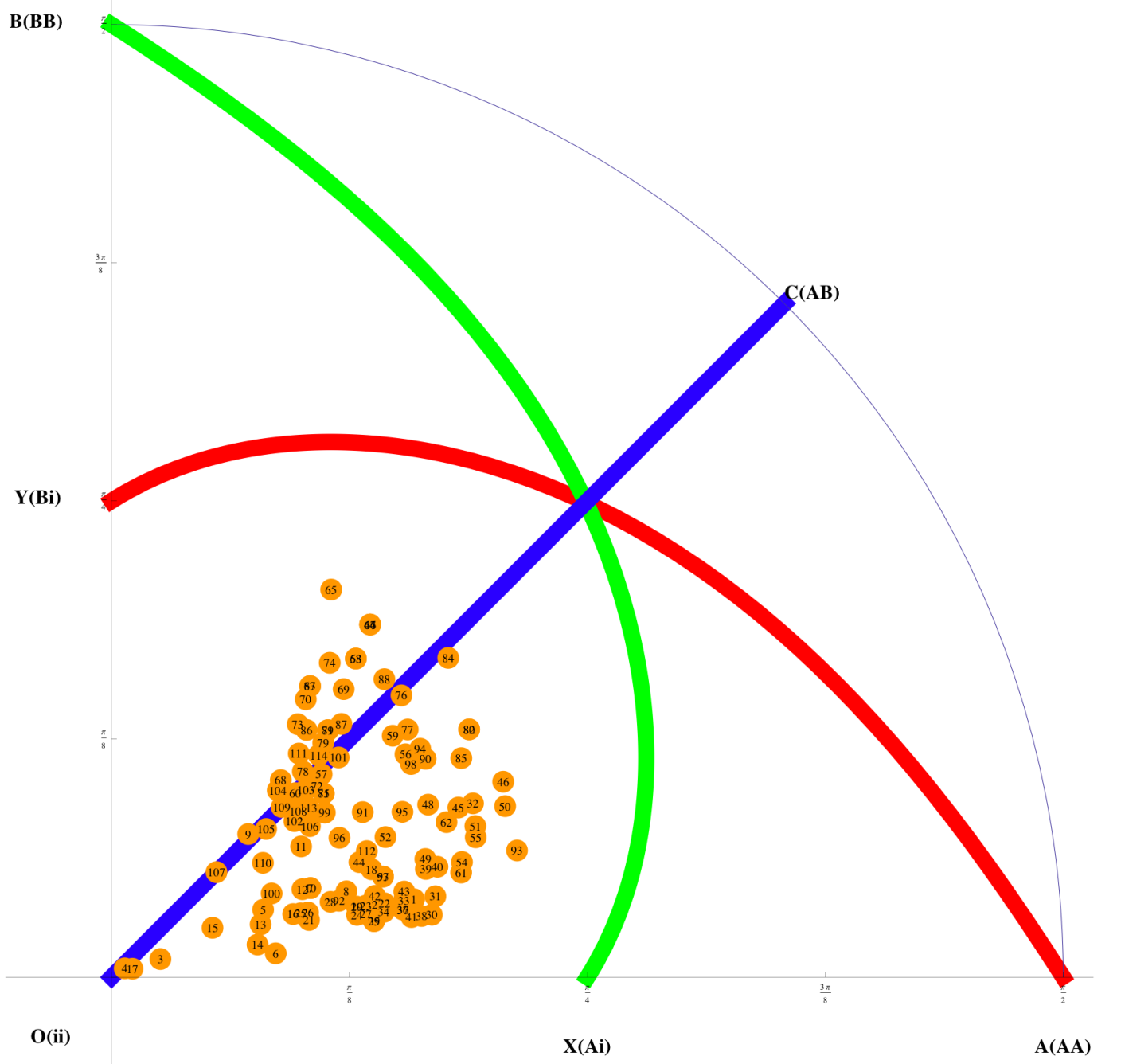


FIG. 10. Similar to FIG.9. The quadrant presented here is a 2-dimensional (θ_1, θ_2) parameterization as in FIG.5. We implement our theoretical prediction of the blood type ratio data of 114 countries in the world from Table V,VI. We plot the theoretical prediction (θ_1, θ_2) distribution of the world ethnic groups from Table V,VI as orange dots. The numbers in the orange dots specify the countries, numbered in the far-left column of Table V,VI.

FIG.11. Quadrant with the Blood Type Population Ratio Distribution by **Countries** from Table V,VI.

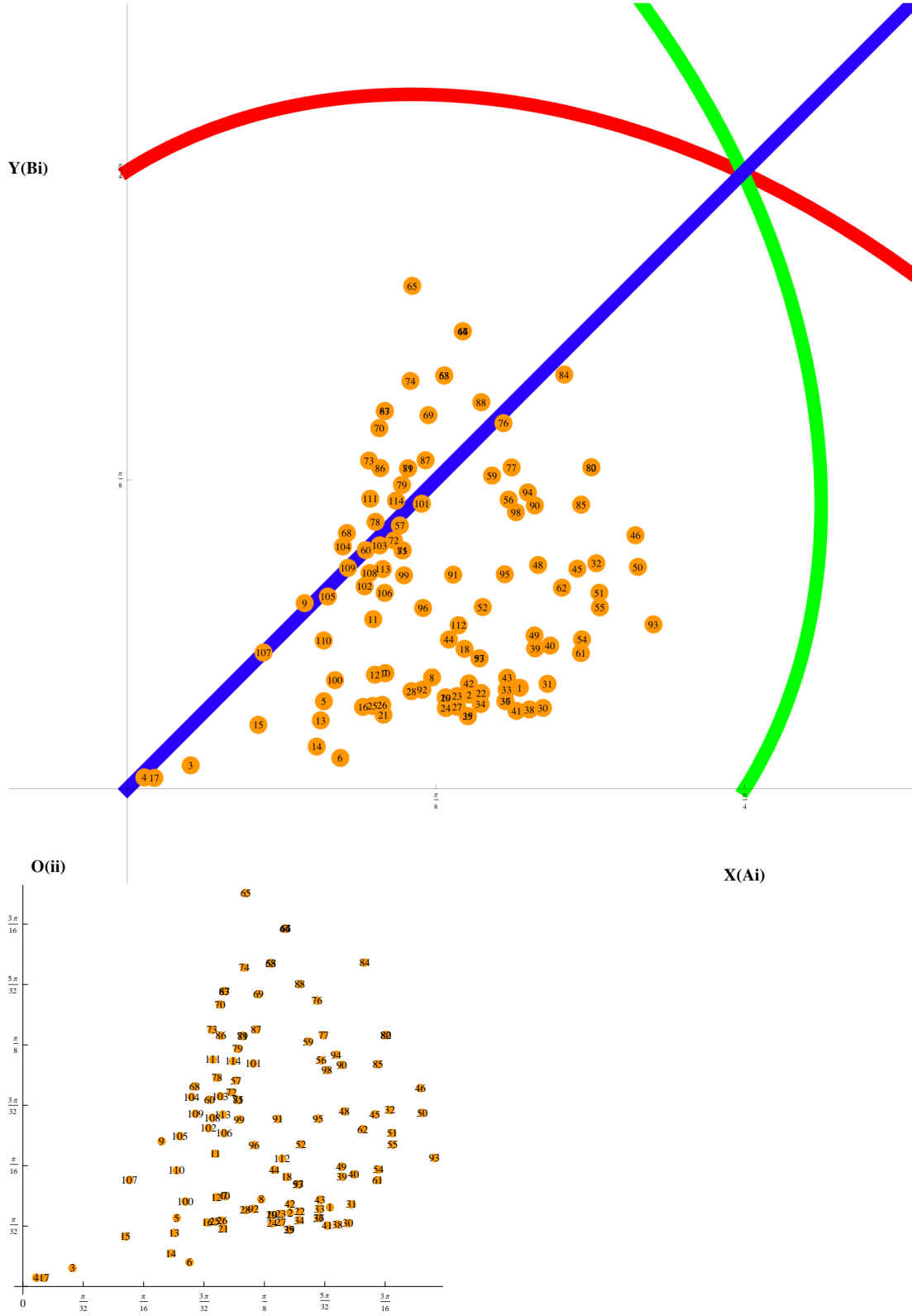


FIG. 11. The zoom-in view of FIG.10. The set up is the same as FIG.10. We implement our theoretical prediction of the blood type ratio data of ethnic groups in the world from Table V,VI.

FIG.12. Blood Type Population Ratio Distribution of both **Ethnics** and **Countries** from Table II,V,VI.

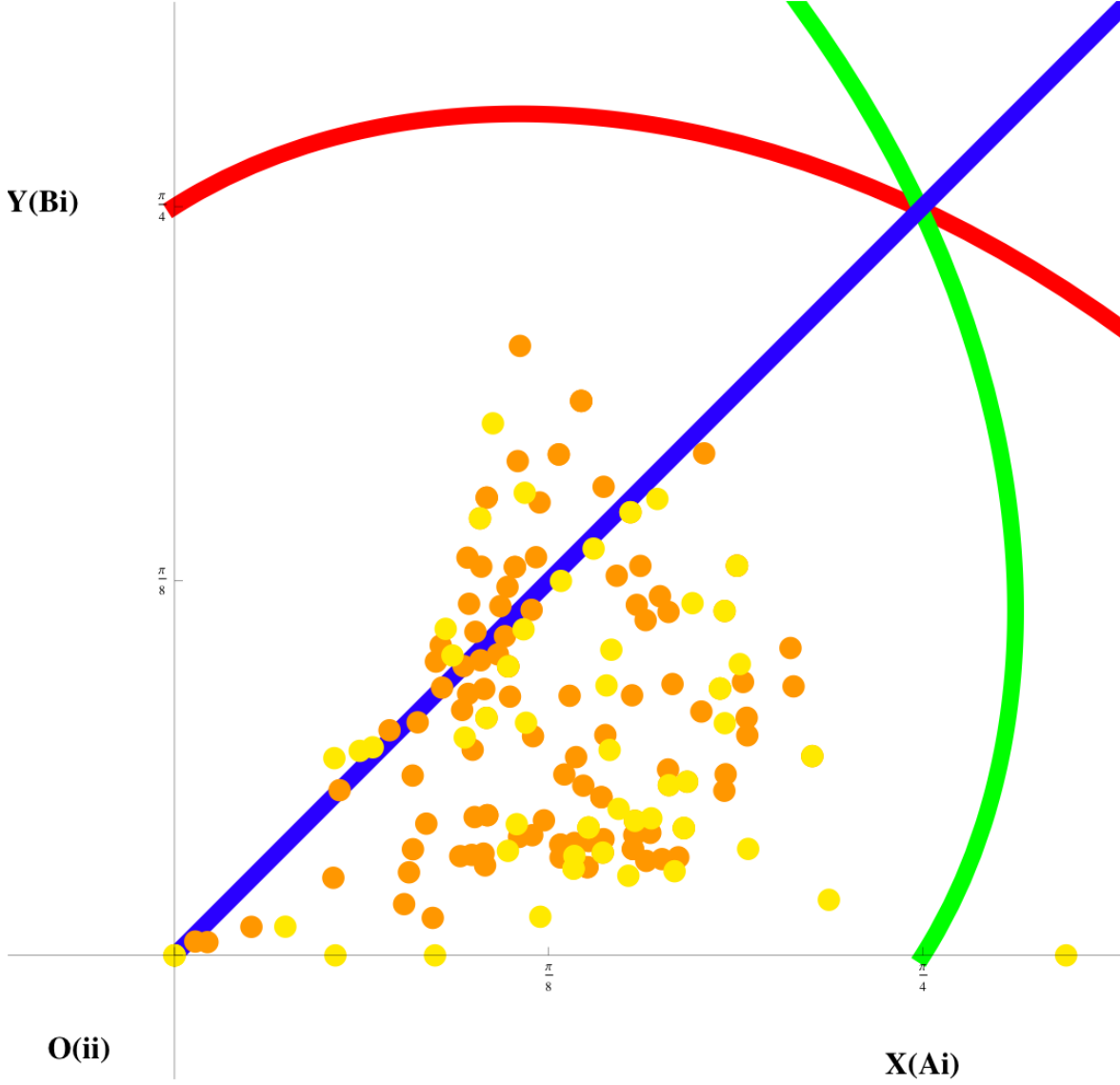


FIG. 12. This is a combined figure of FIG.6 and FIG.7. The quadrant presented here is a 2-dimensional (θ_1, θ_2) parameterization as in FIG.5. We implement our theoretical prediction of the blood type ratio data of ethnic groups in the world from Table II. We plot the theoretical prediction (θ_1, θ_2) distribution of the world ethnic groups from Table II as yellow dots. The numbers in the yellow dots specify the ethnic groups, numbered in the far-left column of Table II. We implement our theoretical prediction of the blood type ratio data of 114 countries in the world from Table V,VI. We plot the theoretical prediction (θ_1, θ_2) distribution of the world ethnic groups from Table V,VI as orange dots.

FIG.13. Geographical Distribution of **World Ethnic Groups** from Table II.

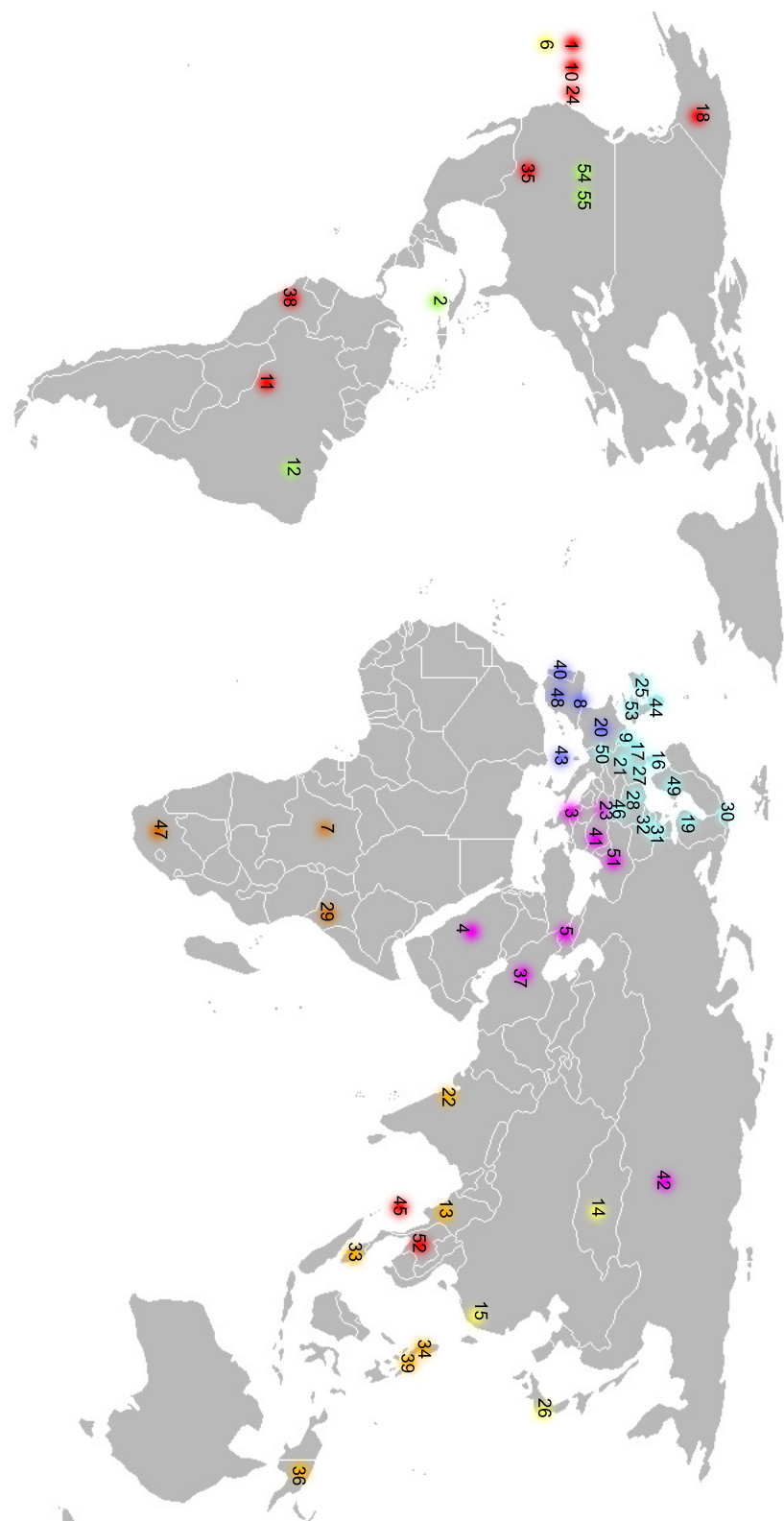


FIG. 13. World map with ethnic group data labeled by the numbers in TABLE II. The numbers in the colored dots specify the ethnic groups, numbered in the far-left column of Table II.

FIG.14. Quadrant with the Blood Type Population Ratio Distribution of **World Ethnic Groups** from Table II.

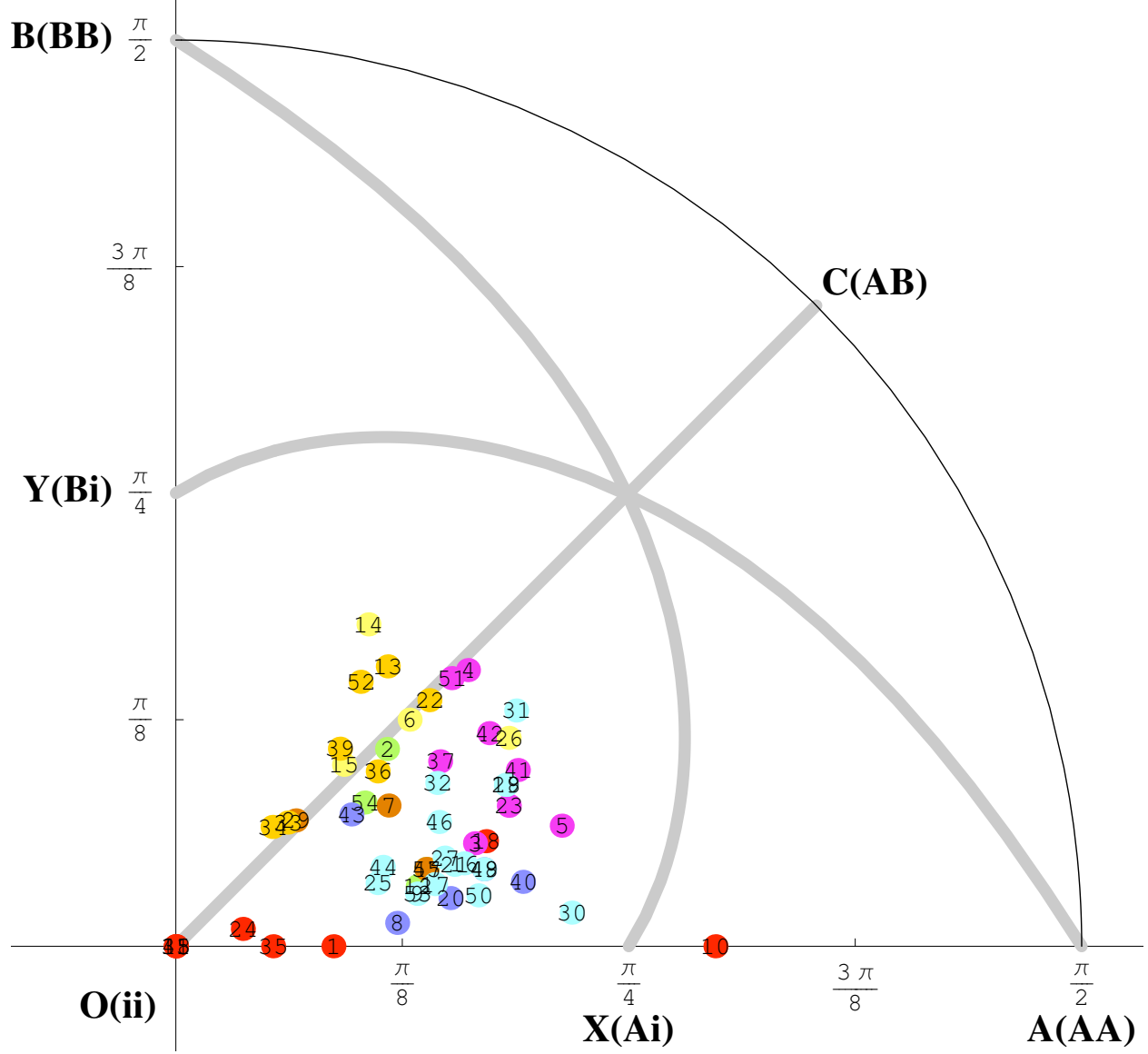


FIG. 14. The quadrant presented here is a 2-dimensional (θ_1, θ_2) parameterization as in FIG.5. We implement our theoretical prediction of the blood type ratio data of ethnic groups in the world from Table II. We plot the theoretical prediction (θ_1, θ_2) distribution of the world ethnic groups from Table II as colored dots. The numbers in the colored dots specify the ethnic groups, numbered in the far-left column of Table II. This FIG.14 is an almost-equivalent figure as FIG.7. The only difference is that we implement the colored dots corresponding to the same colored dots geographically of FIG.13, for a better visualization and comparison to the geographical distribution of ethnic groups in FIG.13.

FIG.14. Quadrant with the Blood Type Population Ratio Distribution of **World Ethnic Groups** from Table II.

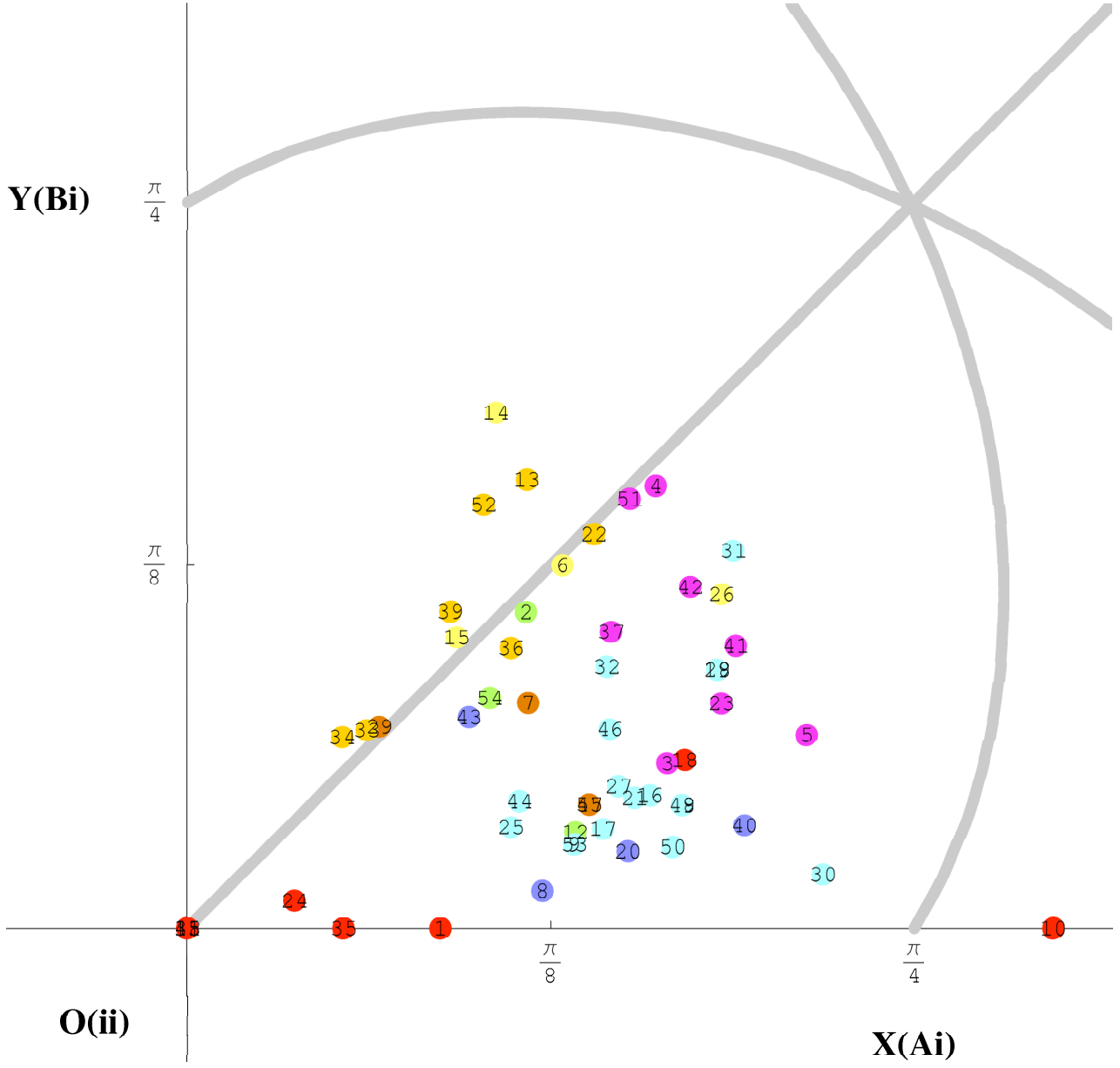


FIG. 15. The zoom-in view of FIG.14. The set up is the same as FIG.14. We implement our theoretical prediction of the blood type ratio data of ethnic groups in the world from Table II.